Diaphragm Control
in Inflated Tool Forming
of Composites

by

Arthur Russell von Waldburg

Submitted to the Department of Mechanical Engineering
in Partial Fulfillment of the Requirements for the Degree of
Bachelor's of Science in Mechanical Engineering

at the

Massachusetts Institute of Technology

June 1997

Signature of Author..
Department of Mechanical Engineering
May 9, 1997

Certified by..
Timothy George Gutowski
Leaders for Manufacturing Professor of Mechanical Engineering
Direc tor Laboratory for Manufacturing and Productivity
Thesis Supervisor

Accepted by..
Peter Griffith
Professor of Mechanical Engineering
Chairman of the Undergraduate Thesis Committee

1

Diaphragm Control
in Inflated Tool Forming of Composites

by

Arthur Russell von Waldburg

Abstract

Advances in material technology have given carbon fiber composites a high strength and stiffness to weight ratios, making them an attractive resource for industry. However, manufacturing parts from sheets of composite laminate is difficult. A forming machine must prevent the laminates from draping over the tool to prevent thickness variations and supply the tensile and shear forces during forming to prevent part wrinkling. The machine must also allow for the easy loading of laminates and removal of formed parts. There are several methods of diaphragm forming in use, the most promising of which is inflated tool forming.

Inflated tool forming relies on a diaphragm inflated around the tool to support the laminate during loading and apply forces during forming. Currently this process does not perform up to the industry's expectations. It may be improved by taking greater control over the diaphragm inflated around the tool.

Three methods of diaphragm control were explored through experimentation: inflating multiple diaphragms, using dense fluid to inflate the diaphragm, and constraining the diaphragm from within. Internal constraints are the most promising method of diaphragm control.

Table of Contents

Introduction

The stiffness and strength to weight properties of make fiber composites attractive to the aerospace and sporting goods industries. Modern composites are made of a reinforcement material and a binder material, in many cases high strength fibers are embedded in a more compliant matrix. An example in widespread use is carbon fiber. Carbon fiber has a tensile strength typically between 3.1 to 5.5 GPa (450 to 800 ksi), a stiffness on the order of 240 GPa (35 Msi), and a specific gravity of 1.7. Thus the fiber is stronger than 7075 aluminum by a factor of 5 to 10, 3.5 times stiffer, and weighs 60 percent as much. These fibers are embedded in a thermosetting polymer such as epoxy. Typical cure temperatures are between 121 and 177° C (250 to 350° F). Unfilled epoxy has a tensile strength of 27.5 to 89 GPa (4 to 13 ksi), a flexural strength of 89 to 144 GPA (13 to 21 ksi), and a specific gravity between 1.11 and 1.40. Recently developed high-toughness epoxies are resistant to damage due to accidental impact. Thus the epoxy effectively binds the fibers together, but adds little in terms of strength or stiffness.

The attractive material properties of fiber composites are offset by their costs. Current costs for carbon fibers are several times to an order of magnitude higher than that of aluminum. The costs differential implies that composite materials will be used in demanding applications where their increased performance justifies their higher cost. However, material cost is only a portion of total product cost. In many applications it has been possible to form composite parts with significantly fewer individual components compared to metallic structures, thus reducing overall costs dramatically. The difficulty here is that industry has yet to find a low cost method of forming many types of composite parts.

Continuous fiber materials is available in partially cured rolls. The rolls represent a single ply of the composite. Many fibers (up to 12,000) with a thickness of 5 to 7 μm (0.0002 to 0.0003 in) are gathered together in the manufacturing process to form

a tow or yarn. These tows are coated with the matrix material in a process called prepregging and partially cured to form a ply, or sheet of composite. These sheets contain a number of tows through their thickness. Typically a ply is 60 percent fiber by volume. To prevent unwanted curing, these rolls of composite must be kept refrigerated until used. During prepreg lay-up individual plies of prepreg are laid together, using a tool to control part geometry. The plies are laid in a pattern determined by classical lamination theory such that their angles between their respective fibers result in the desired strength and stiffness characteristics of the product. Thus strong, thick parts consist of many plies.

Automating the lay-up process has been difficult due to the in-plane shear forces necessary to prevent wrinkling as each ply is formed over the tool. The combination of bending and shear forces necessary to form an align fiber ply to any complex shape 'topologically' equivalent to a flat sheet were described by S. Tam and T. Gutowski in their 1990 paper. In a special case, the in plane shear forces on a single fiber, Γ_{12}, can be described by[1]

$$\Gamma_{12} = \int_{C_3} k_g ds = -\iint_R KdA = -K_T(R) \tag{1}$$

where Γ_{12}, the in-plane shear, along a fiber path, C_3, over the geodesic curvature of the arcs, k_g, is related to the total curvature, K_T, over the region R. These paths are described in Figure 1. If the necessary shear forces are not achieved, the composite wrinkles during forming. Wrinkles are undesirable because they detract from the strength of composite materials and act as stress risers.

Automated forming must also create precise parts to be feasible. This is achieved by controlling the shape variables during forming. If the part shape is not constant, the imprecision drives up the price of assembly by requiring unique shims to be placed

---

[1] From Albert S. Tam and T. Gutowski, "The Kinematics for Forming Ideal Aligned Fiber Composites into Complex Shapes," Composites Manufacturing Vol 1 No 4 December 1990
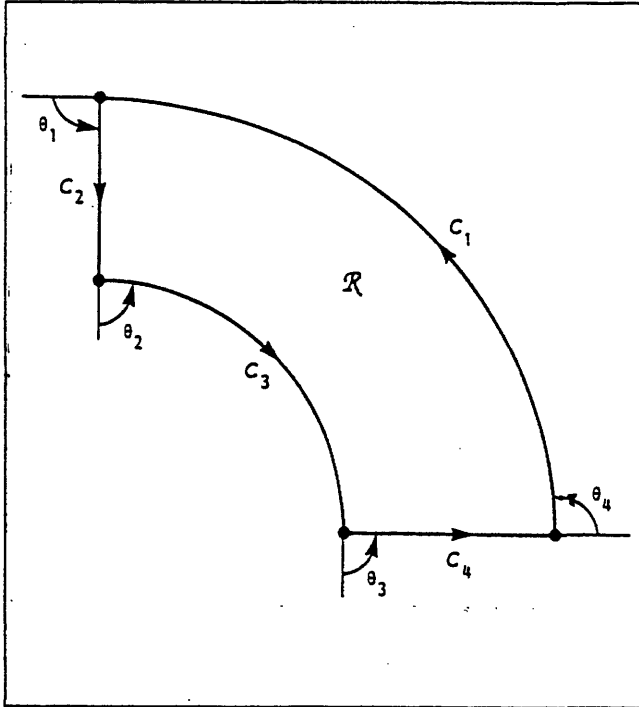
between parts. The three current forming machine designs each embody different trade-offs between wrinkle prevention and part precision.

Drape Forming

The drape forming process creates parts by pulling the laminate over a tool using a single diaphragm. The laminate is laid on top of the tool, then a diaphragm is used to seal the machine as shown in Figure 2. Pulling a vacuum in the chamber causes the diaphragm to form the prepreg over the tool. The top loading machine allows laminates to be created through successive runs and the finished part to be removed easily. However, drape forming does not work well for large parts because the laminate droops over the tool before forming, creating thickness variations by stretching the laminate unevenly. One way to prevent drooping is to invert the process. But, as Figure 3 shows, inversion makes it necessary to lift the tool before loading the machine with prepreg, or removing the finished
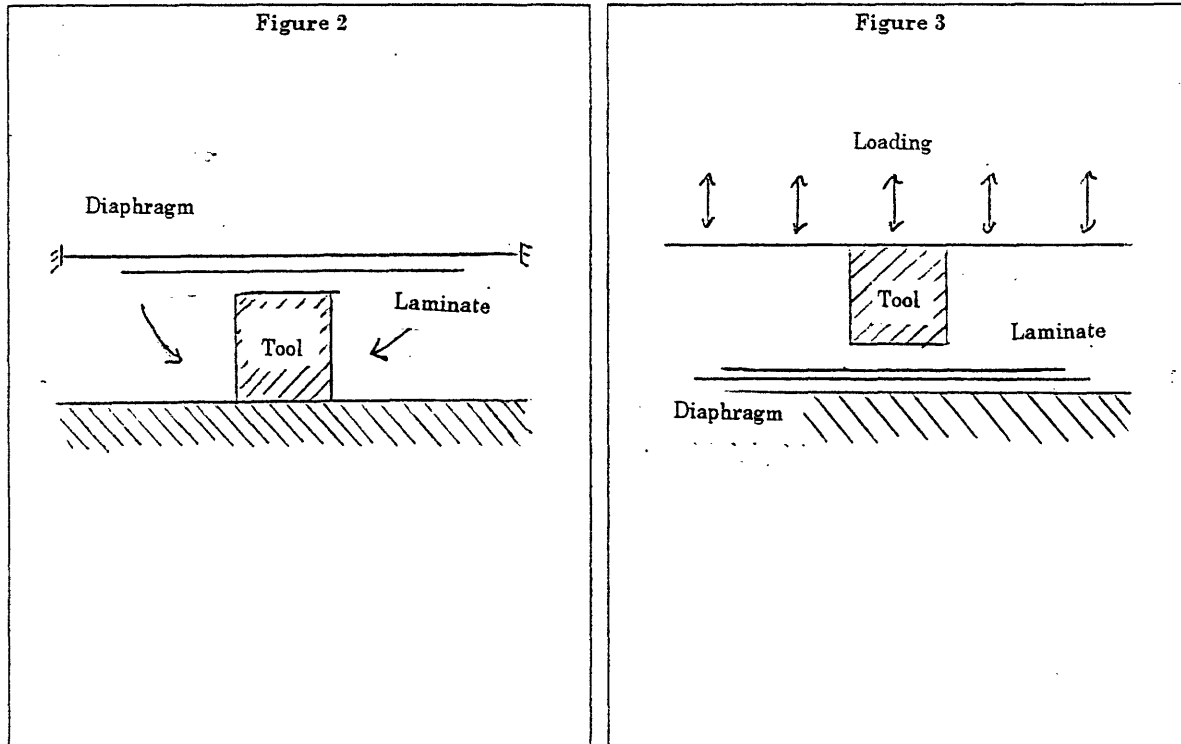
Figure 2: The drape forming machine uses a single diaphragm to mold parts over a tool. There drooping inherent in loading this machine is removed by inverting the process as shown in Figure 3. However, this inversion necessitates the movement of the tool during loading and unloading of the machine.

product. Repeatedly lifting large tools is cumbersome and time consuming.

Double Diaphragm

A way to support the laminate prior to forming is with a double diaphragm. In this machine, the laminate is sandwiched between two diaphragms as shown in Figure 4. The lower diaphragm prevents the prepreg from drooping and the sandwich effect supplies additional shear during forming, making it possible to form thicker laminates (more plies) with each run. Because it is between the laminate and the tool, the second diaphragm also makes the parts imprecise by introducing its thickness as a variable in forming. Any addition plies added with this machine in subsequent runs are done with drape forming because the lower diaphragm is trapped between the laminate and the tool. The lower diaphragm also makes it difficult to remove formed parts from the machine without damaging them.

Figure 4: The double diaphragm machine supports the laminate with a second diaphragm during loading. Sandwiching the laminate between diaphragm increases the shear force applied during forming, preventing wrinkles, but makes the parts imprecise by trapping the lower diaphragm between the laminate and the tool.
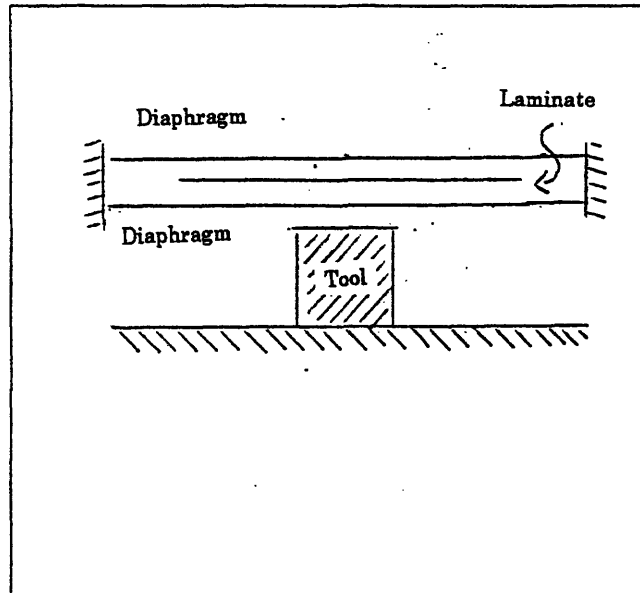
Inflated Tool

The most promising method is inflated tool forming. In this process, a diaphragm is inflated to support the laminate as it is loaded into the machine. Then a second diaphragm is placed on top of the laminate. In theory, pulling a vacuum between the diaphragms will provide the sandwich effect of double diaphragm forming while providing the easy loading/unloading and precision of drape forming. In practice, the lower diaphragm does not inflate to completely fill the space around the tool. The rounded diaphragm inflation observed (Figure 5) provides incomplete support during loading and may even pinch the laminate, creating wrinkles during forming[2].

Inflated tool forming may be improved through better control of the lower diaphragm. Ideally the diaphragm would inflate to fill the entire chamber, providing a flat surface to support the laminate during loading. Then apply shear forces to the laminate through tension in its surface as it deflated as seen in Figure 6. The three methods of control I examined are inflation with dense fluid, multiple diaphragm inflation, and inflation against internal constraints.

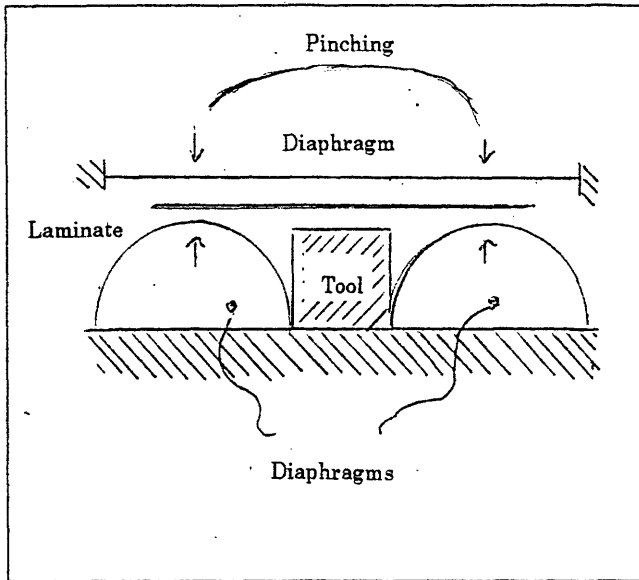---

[2] from research done by Paul Llamas

Figure 5: In inflated tool forming, a diaphragm is inflated around the tool to provide support during loading and additional shear forces during forming. In practice, the inflated diaphragm provides only a point of support, and does not effectively sandwich the laminate. In fact, its rounded shape may pinch the laminate during forming, thus *creating wrinkles*

Figure 6: An ideal inflated tool machine provides a flat bed onto which the laminate is loaded, and sandwiches the laminate, providing additional shear forces during forming.
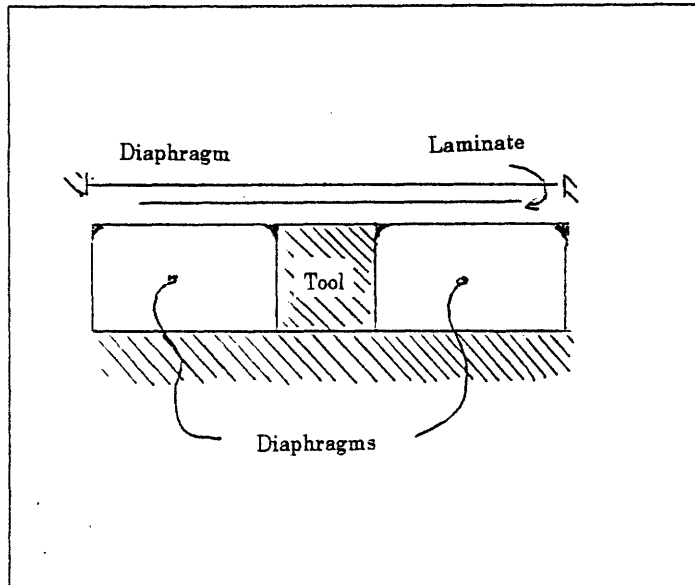
Controlling the Diaphragm

An uncontrolled diaphragm deforms in response to the stresses created by an evenly distributed lateral load (pressure) on its surface. Neglecting changes in diaphragm thickness, the stresses, σ, in the diaphragm can be modeled as the stresses in a plate under evenly distributed load[3]:

$$\sigma = k_1 \frac{wx^2}{t^2} \tag{2}$$

The resulting deformation, y, is

$$y = k_2 \frac{w(R - |x|)^4}{Et^2} \tag{3}$$

In both equations w is the evenly distributed load (pressure), t is the thickness, and x denotes the position on the diaphragm. E is the young's modulus of the diaphragm. The definitions of R, k_1, and k_2 are determined by the shape and size of the diaphragm as well as the manner in which its edges are anchored. For a circular diaphragm fixed on all edges (Figure 6), R denotes the radius, k_1=0.71, and k_2=0.171. Additional definitions of R and the empirical constants (k_1 and k_2) are in Appendix A.
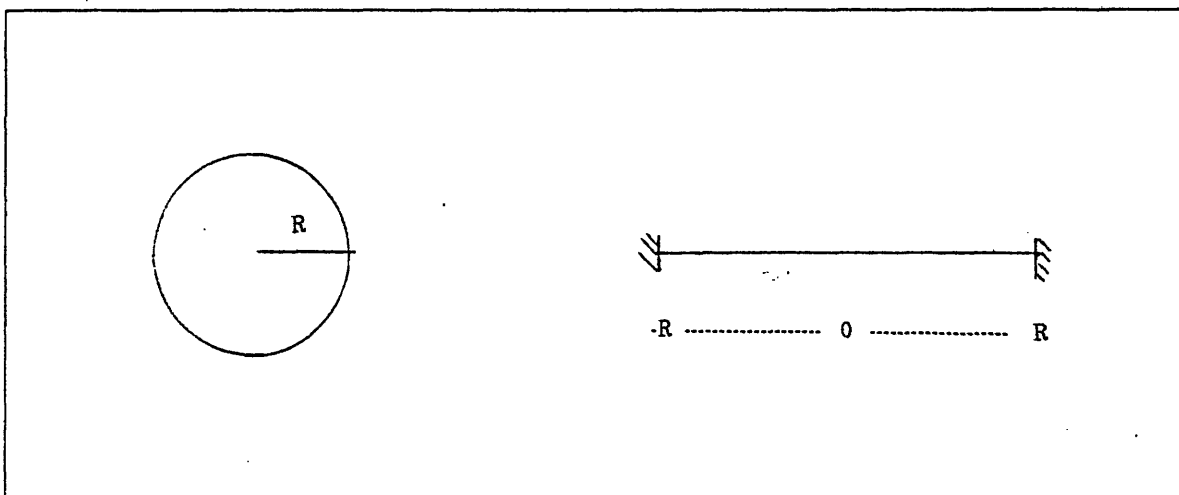
Figure 6: A circular diaphragm fixed at the edge.

---

[3] From **Mark's Standard Handbook for Mechanical Engineers** 10th Edition pg 5-48

Diaphragm control is needed to provide a flat surface to support the laminate during loading of inflated tool machines, and to exert shear forces on the laminate through tension in the diaphragm.

Fluid Inflation

Using a dense fluid to inflate the diaphragm flattens the diaphragm deformation by exerting an uneven load on the diaphragm surface. When filled with a dense fluid, the pressure, P, at any point on the diaphragm will be the sum of a base pressure, P_o, and the height of the fluid column, h, at that point

$$P = P_o + \rho h \tag{4}$$

Approximating the height as the difference between the maximum height and the height at point x in an uncontrolled diaphragm yields:

$$h = k_2 \frac{P_o R^4}{Et^3} - k_2 \frac{P_o x^4}{Et^3} = k_2 \frac{P_o}{Et^3}(R^4 - x^4) \tag{5}$$

Then substituting Equation 5 into Equation 4 gives the pressure in the diaphragm as a function of x:

$$P = P_o + \rho k_2 \frac{P_o}{Et^3}(R^4 - x^4) \tag{6}$$

Substituting Equation 6 into Equation 3 gives the deformation of a fluid filled diaphragm

$$y = k_2 \frac{(R-x)^4}{Et^3}[P_o + \rho k_2 \frac{P_o}{Et^3}(R^4 - x^4)] \tag{7}$$

This is shown in Figure 7. The degree to which diaphragm inflation is flattened is determined by the ratio of fluid density to the diaphragm's Young's modulus. Higher ratios yield greater flattening of the diaphragm.
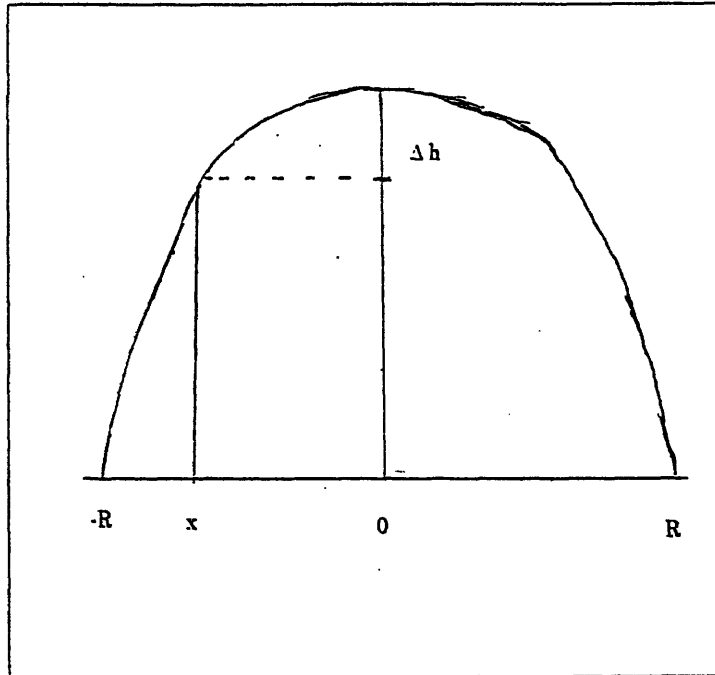
Multiple Diaphragms

With Prof. Christine Bordonaro, the use of multiple diaphragms in the lower

portion of the inflated tool forming machine was developed. When diaphragms expand

into the same space they are constrained and deflected. Figure 8 highlights the contested

volume between diaphragms. The force one diaphragm exerts on another is determined

by the internal pressure, the relative elasticity (determined by thickness of similar

diaphragms), and the friction between the diaphragms. Due to its complexity, this model

was left to be determined empirically.
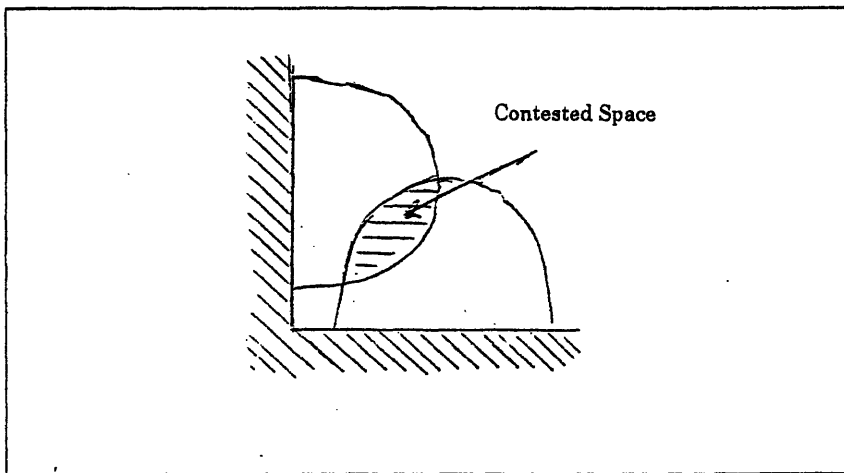
Figure 8: When
perpendicular
diaphragms are inflated,
they expand into the
same space. The
interaction at this point
is determined by
relative elasticity and
friction between the
diaphragms

Internal Constraints

Internal constraints limit the vertical deformation of the diaphragm. A pattern of constraints across the diaphragm will define the surface of the diaphragm when the length of the constraint at point x, l_x, is less than the uncontrolled deformation of the diaphragm at that point. Thus control is exerted over the diaphragm surface when

$$l_x < k_2 \frac{P_o x^4}{Et^3} \tag{7}$$

Vertical constraints of the same length will create a flat surface on the diaphragm, as seen in Figure 9. Figure 10 illustrates that this method of diaphragm control can be

Threads
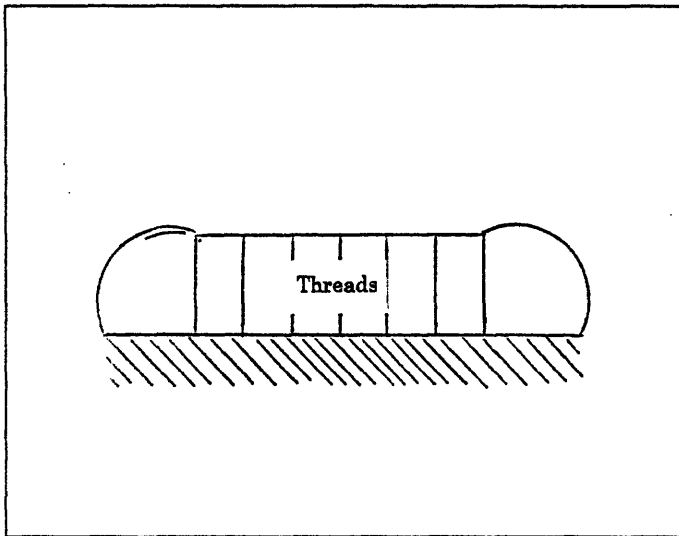
Figure 9: A flat surface being dictated to a diaphragm via internal constraints of the same length.

modeled as two uncontrolled diaphragms mounted on slopes which connect a raised platform to a fixed base. The expansion of these two diaphragms can be described by

$$y_i = k_2 \frac{P_o (R - |x_i|)^4}{Et^3} + \tan \alpha_i d_i \tag{8}$$

where α is the angle between the fixed base and the slope to the raised platform, x is the position on the diaphragm, and d is the distance between the point where the diaphragm is fixed to the base and the point at which it is simply supported by the platform. The uncontrolled portions of the diaphragm should expand to fill any gaps between the tool and the controlled portion.
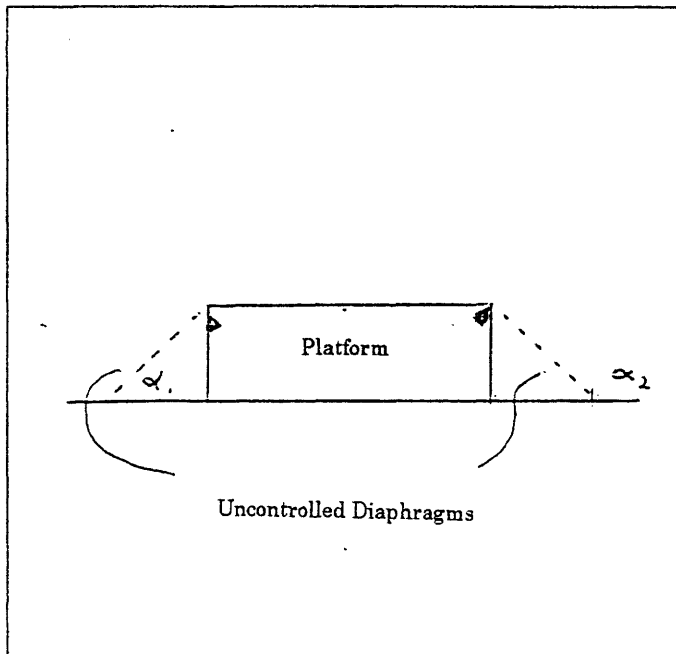
Figure 10: Internally constrained diaphragms can be modeled as a raised platform between two inclined, uncontrolled diaphragms.

The effectiveness of these methods at controlling the diaphragm during inflation and deflation was determined through a series of experiments.

Testing Procedure

The same apparatus was used in each test of diaphragm control. A small model of a forming machine, shown in Figure 11, was used to house the experiments. The box has holes drilled in the bottom and one side. Diaphragms were place over these holes and sealed to the box by bolting aluminum collars over them. Air or fluid was supplied to the diaphragms through the holes. The diaphragms used in these experiments were $1/50$ and $1/16$ inch thick latex. Latex has a Young's modulus of about 6.89 Pa (10^{-3} psi). Set at 0.7 Pa (10 psi), the lab's air supply was used as a pressure source. Each test was documented on video.
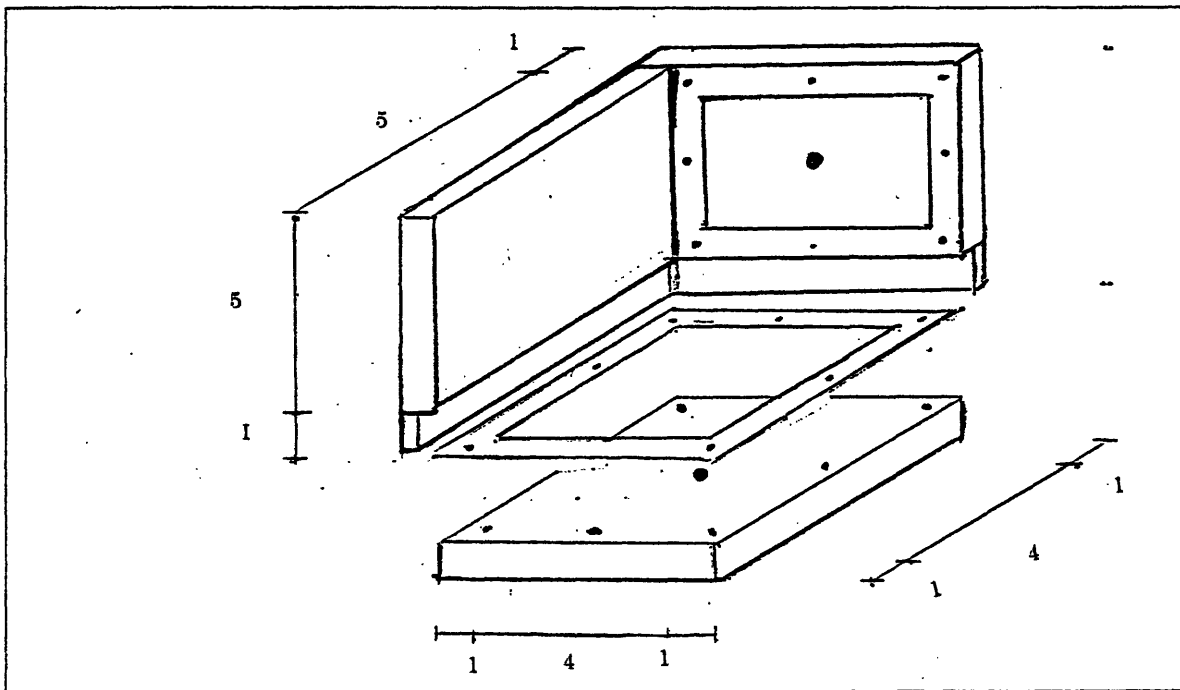
Figure 11: An exploded view of the testing apparatus showing the input holes, sealing collars, gaskets and bolts.

Fluid Inflation

The horizontal diaphragm was inflated with fluid by pressurizing a water-bottle connected to the hole at the bottom of the test apparatus. As shown in Figure 12, a straw ensures that the test fluid rather than the air used to pressurize reservoir is
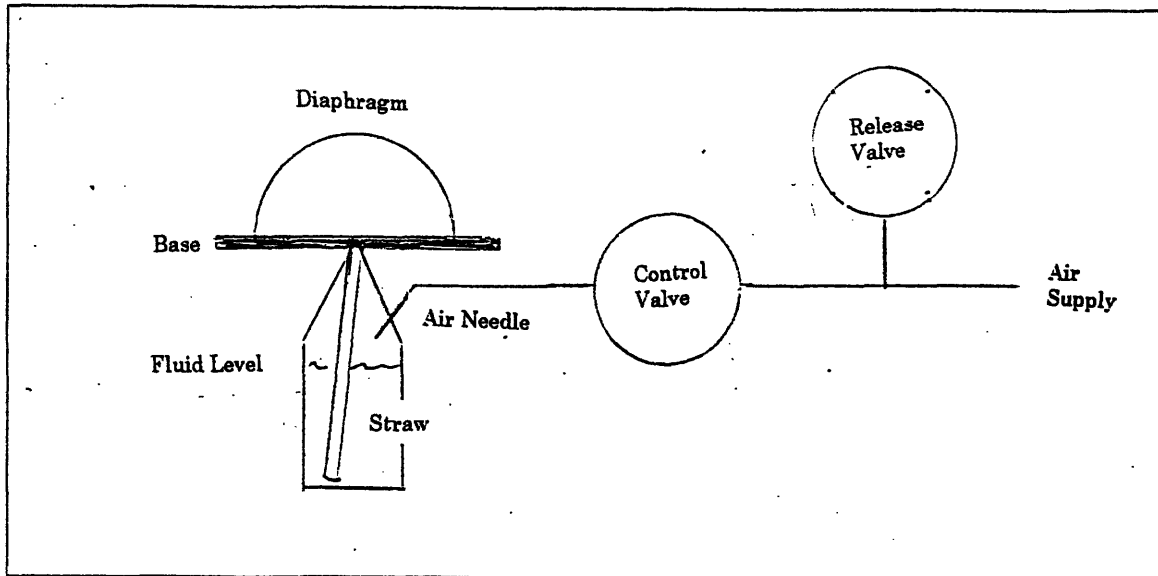
Figure 12: Fluid is forced into the horizontal diaphragm through a straw when the reservoir (water bottle) is pressurized with air.

pumped into the diaphragm. The diaphragm was inflated with water, using air as a control. The densities of these fluids are in Table 1. Inflation of the diaphragm was limited by the volume of the water bottle.

Fluid	Air	Water
ρ (kg/m^3)	24	1,000

Table 1: Densities of fluids used for diaphragm inflation.

Multiple Diaphragms

Tests of control using perpendicular diaphragms examined the effect of relative thickness, inflation order, and friction on the diaphragm interaction. Connecting air hoses to both the horizontal and vertical diaphragms through additional valves, see Figure 13, provided control over the inflation sequence. The tests listed in Table 2 were performed, using different combinations of diaphragm thickness and inflation sequence then repeated, using petroleum jelly to reduce the friction between the diaphragms. The dry tests had to be performed before the low friction tests because the petroleum jelly degraded the latex diaphragms.

16
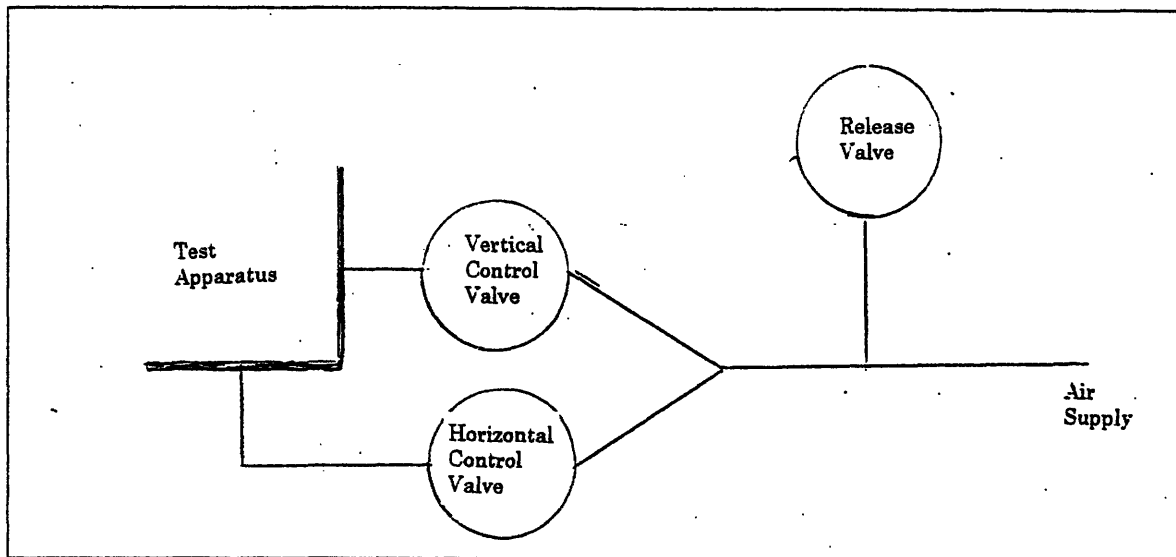
Figure 13: The air supply is split and directed to the horizontal and vertical diaphragms through two additional valves.

Test #	Horizontal Thickness (in)	Vertical Thickness (in)	Inflation Order	Interface
1	$1/50$	$1/50$	Together	Dry
2	$1/50$	$1/50$	Horizontal First	Dry
3	$1/50$	$1/50$	Vertical First	Dry
4	$1/50$	$1/50$	Together	Petroleum
5	$1/50$	$1/50$	Horizontal First	Petroleum
6	$1/50$	$1/50$	Vertical First	Petroleum
7	$1/16$	$1/50$	Together	Dry
8	$1/16$	$1/50$	Horizontal First	Dry
9	$1/16$	$1/50$	Vertical First	Dry
10	$1/16$	$1/50$	Together	Petroleum
11	$1/16$	$1/50$	Horizontal First	Petroleum
12	$1/16$	$1/50$	Vertical First	Petroleum
13	$1/50$	$1/16$	Together	Dry
14	$1/50$	$1/16$	Horizontal First	Dry
15	$1/50$	$1/16$	Vertical First	Dry
16	$1/50$	$1/16$	Together	Petroleum
17	$1/50$	$1/16$	Horizontal First	Petroleum
18	$1/50$	$1/16$	Vertical First	Petroleum

Table 2: Tests carried out with perpendicular diaphragms

Internal Constraints

Internal constraints were fabricated by sewing the diaphragms to a stiff base using nylon cord. During the sewing process, the diaphragm was separated from the

base by a flat piece of Styrofoam. This is shown in Figure 14. The stitching was then painted over with pre-vulcanized liquid latex. After the diaphragm was sealed, the Styrofoam was dissolved using acetone. Without the Styrofoam, the diaphragm lays flat against the base until pressurized as seen in Figure 17.
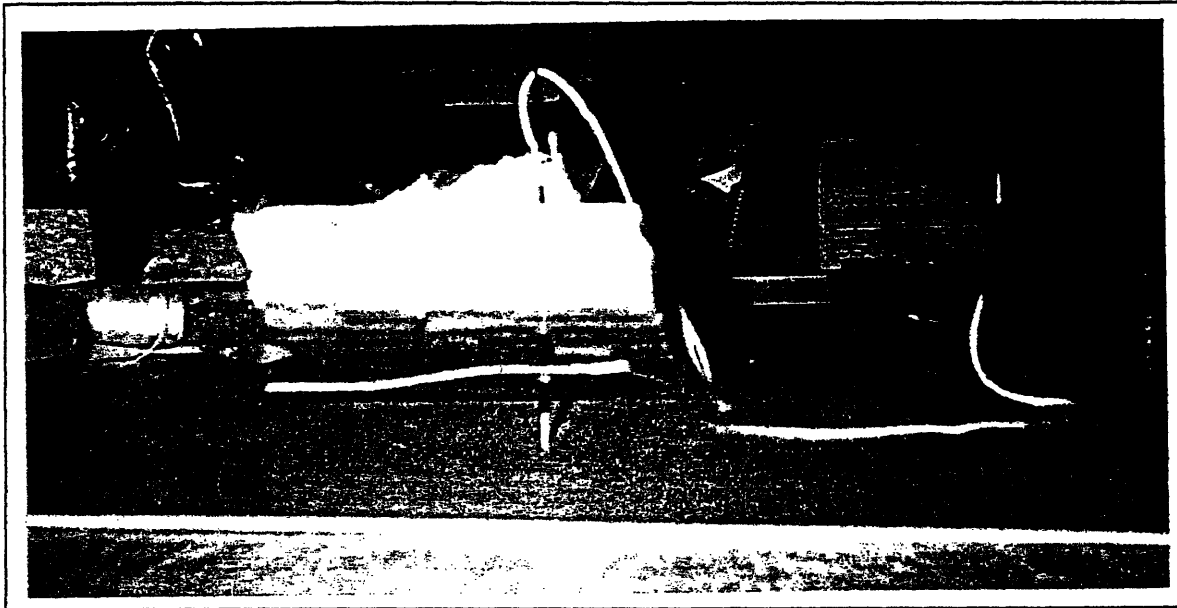
Figure 14: Nylon threads were stitched through foam into a stiff tagboard base using a sharpened darning needle with a hole drilled in it.
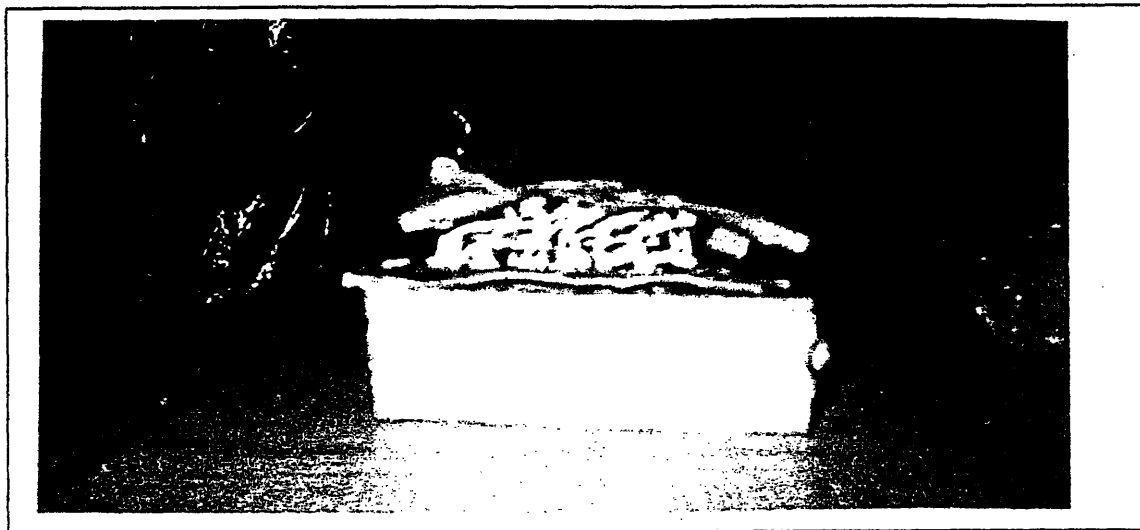
Figure 15: Dissolving the foam with acetone leave the diaphragm able to be compressed against the stiff base, yet constrained vertically by the nylon threads.

Several problem arose to complicate the process. Styrofoam dissolved into a sticky taffy-like substance, necessitating its replacement with poly-urethane foam. Experiments showed that the poly-urethane foam dissolved into a slimy substance resembling wet paper, making it much easier to remove from between the threads. Then the pre-vulcanized liquid latex did not adhere well to the latex diaphragms at high pressure, nor did the threads remain parallel when the diaphragms were inflated, as illustrated in Figure 16. These problems were solved by stitching fabric to the stiff base through the poly-urethane foam, then form a diaphragm on top of the stitching, thus incorporating the stitching and fabric into the diaphragm. This process uses the inextensible properties of the fabric to keep the diaphragm from expanding between the threads, keeping them parallel and using one-step diaphragm forming to creates diaphragms able to withstand higher pressures. One such diaphragm is shown in Figure 17. In this process, it is important to prevent thickness variations in the diaphragm and eliminate bubbles in the liquid latex. Both of these faults create weak points in the diaphragm.

Figure 17: The diaphragm expands between the stitches, bringing them out of alignment. The dispersed threads created large 'air mattress' effects on the surface of the diaphragm.

Once fabricated, the internally constrained diaphragms were placed on the horizontal surface of the testing apparatus and inflated.
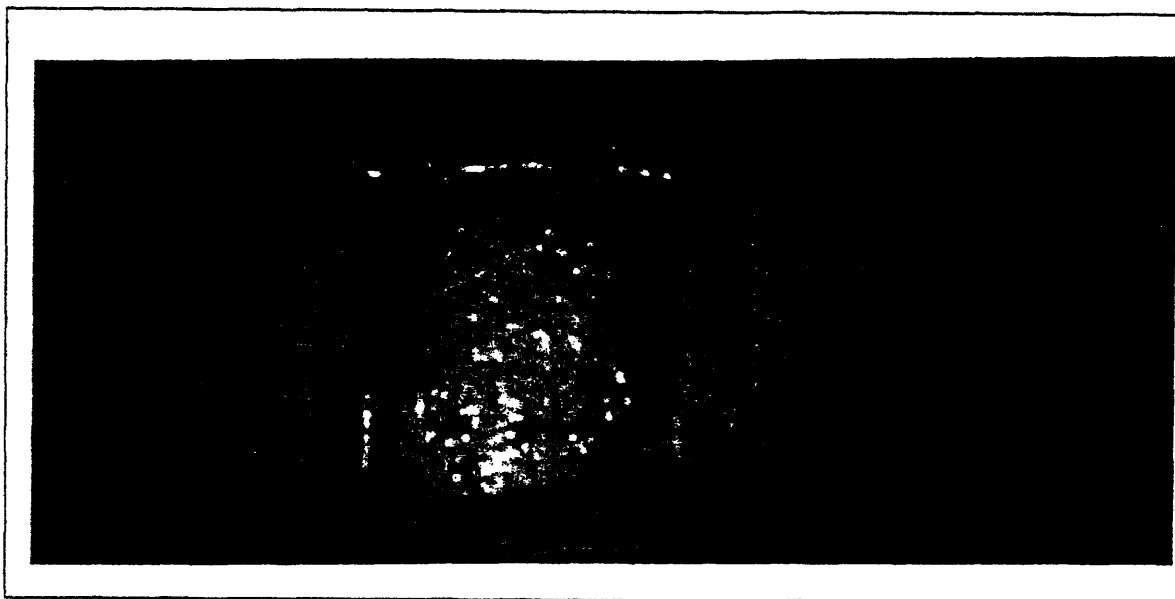
Figure 18: A diaphragm incorporating stitching and cloth into its fabrication.

Results

The three methods of controlling diaphragms met with varying degrees of success. Included here are the most dramatic stills from the video documentation. Stills from all the tests can be found in Appendix B.

Fluid Inflation

Using fluid to inflate the horizontal diaphragm did not yield dramatic results. The diaphragm was only slightly flatter when filled with water than when filled with air. This can be seen by comparing Figures 19 and 20. The control over the diaphragm would increase if the linear effect of hydrostatic pressure dominated the exponential expansion of the diaphragm.
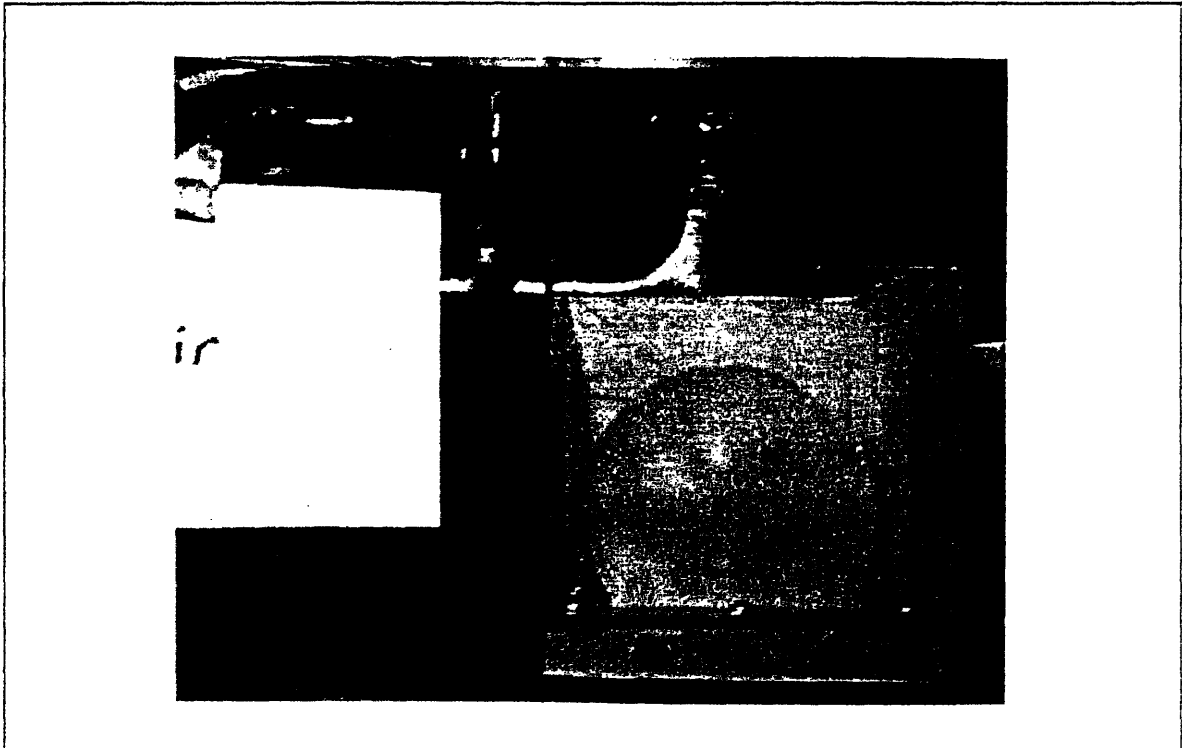
Figure 19: Diaphragm filled with air. Density of air is 24 kg/m^3
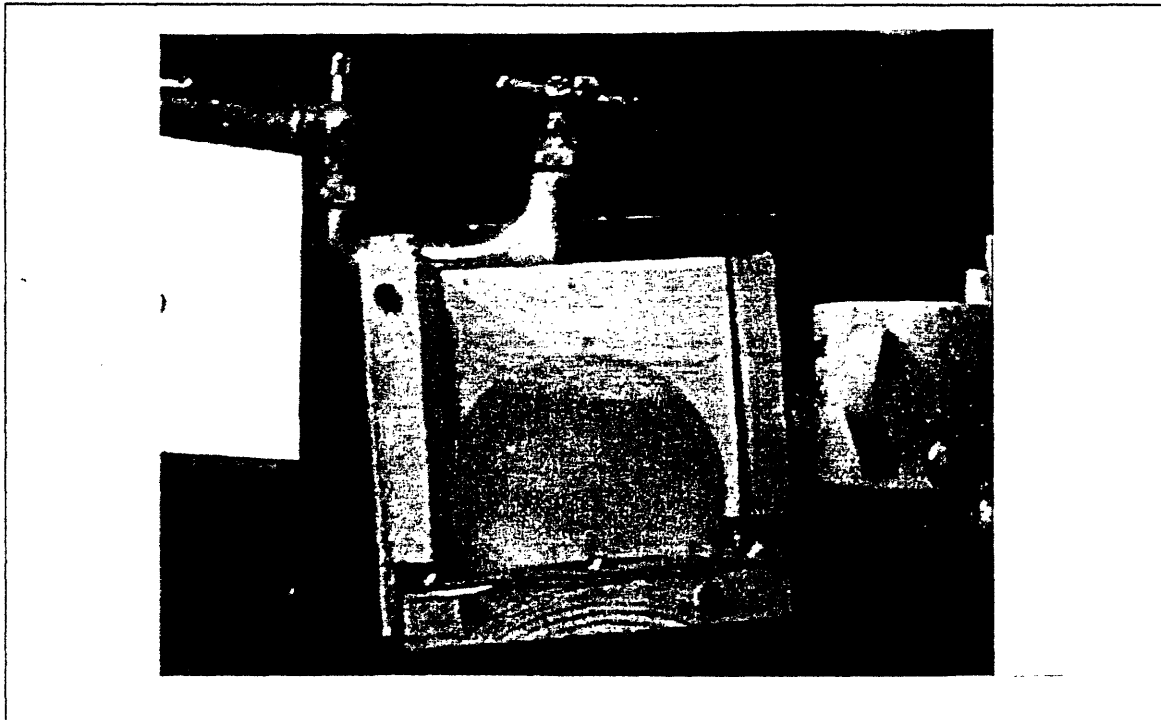
Figure 20: Diaphragm inflated with water. Density of water is 1000 kg/m^3

Multiple Diaphragms

Multiple diaphragm inflation yielded some interesting results. When the

diaphragms are the same thickness (have the same elasticity) inflation order is a

dominant factor in their interaction. The diaphragm which is inflated first is

deflected by the second diaphragm as seen by comparing Figures 21 and 22.
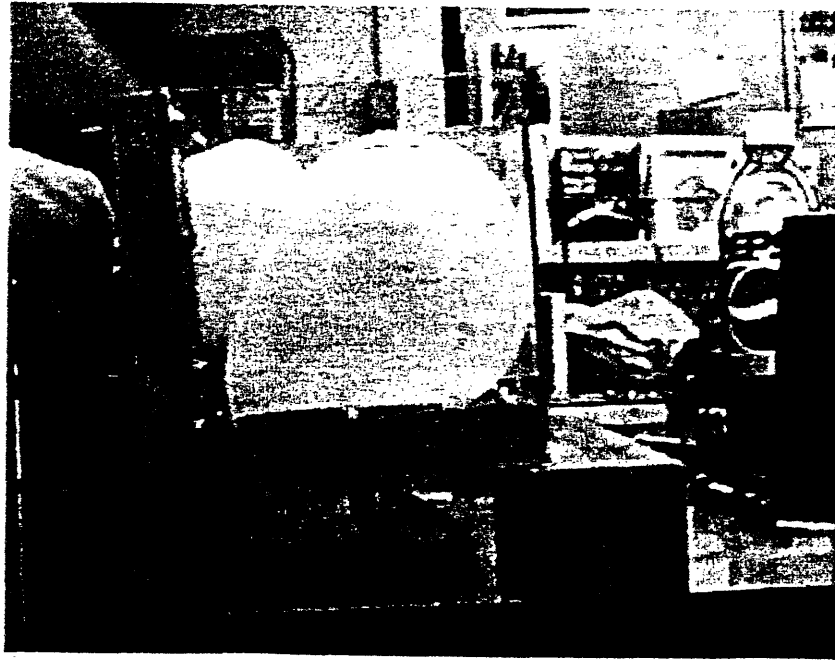
Figure 21: Diaphragms of the same thickness with the horizontal diaphragm inflated first
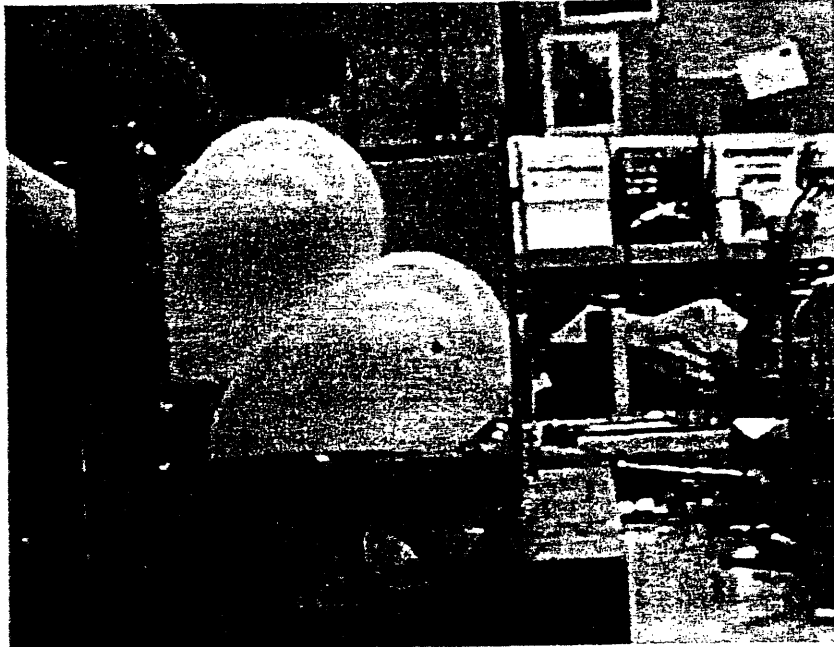
Figure 22: Diaphragms of the same thickness with the vertical one inflated first

Though inflated at the same pressure, the thicker diaphragm displaces the thinner diaphragm, regardless of the inflation order. However, Figures 23 and 24 show that when the thicker diaphragm is inflated first, the thinner diaphragm inflates around it, but when the thicker diaphragm is inflated second, the thinner diaphragm is pushed aside. The dry, horizontal first test with $t_H = \frac{1}{30}"$ $t_V = \frac{1}{16}."$ seen in Figure 24, shows the most dramatic effect on diaphragm shape with the minimum upward deflection. This test was the closest that multiple diaphragm inflation came to creating a flat loading surface while almost completely filling the expansion chamber.

Figure 23: Diaphragm interaction with the thicker, vertical diaphragm inflated first.

Figure 24: The diaphragms nearly fill the expansion chamber with nearly no upward deflection when the thicker, vertical diaphragm is inflated second

Internal Constraints

The internally constraints were very successful at controlling the surface of the diaphragm. Though the stitched diaphragms exhibited dramatic expansion between the threads, The diaphragms with imbedded fabric were remarkably flat on top as shown in Figure 25. The uncontrolled portions expanded to fill the chamber. This expansion is shown against a tool in Figures 26 and 27.
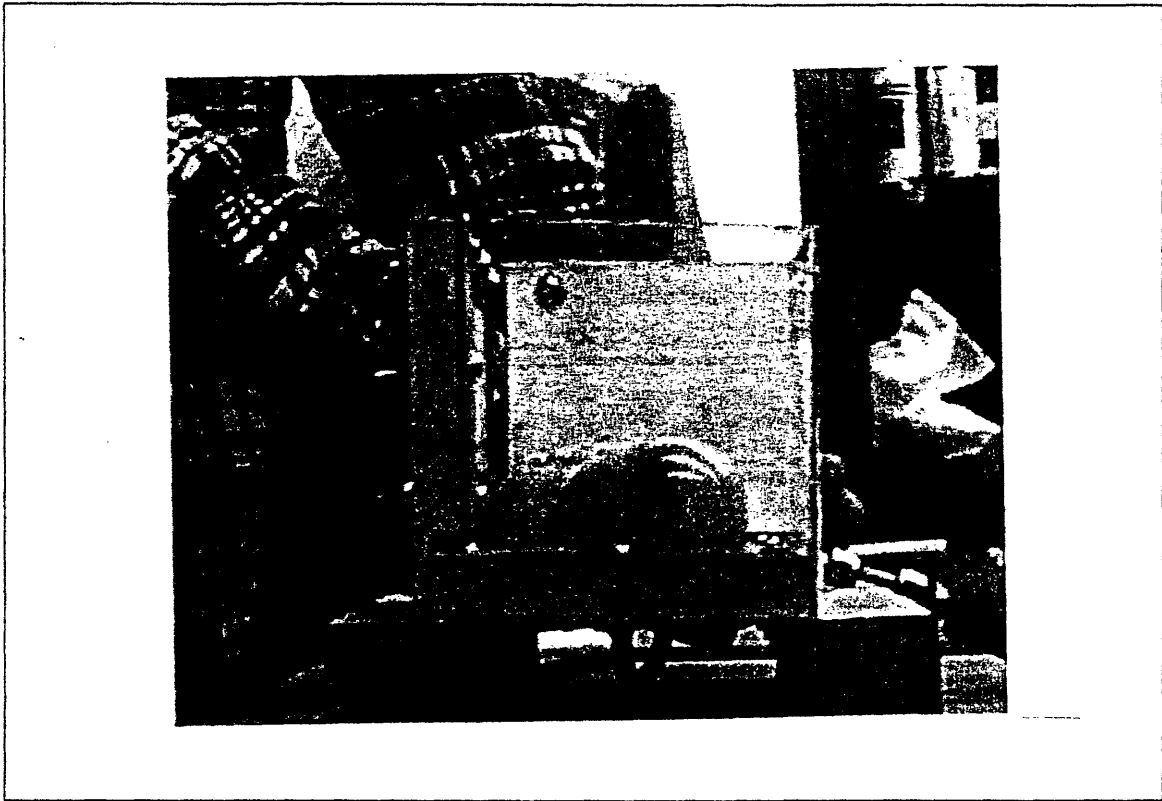
Figure 25: Internally constrained diaphragms with imbedded fabric were remarkably flat on top.
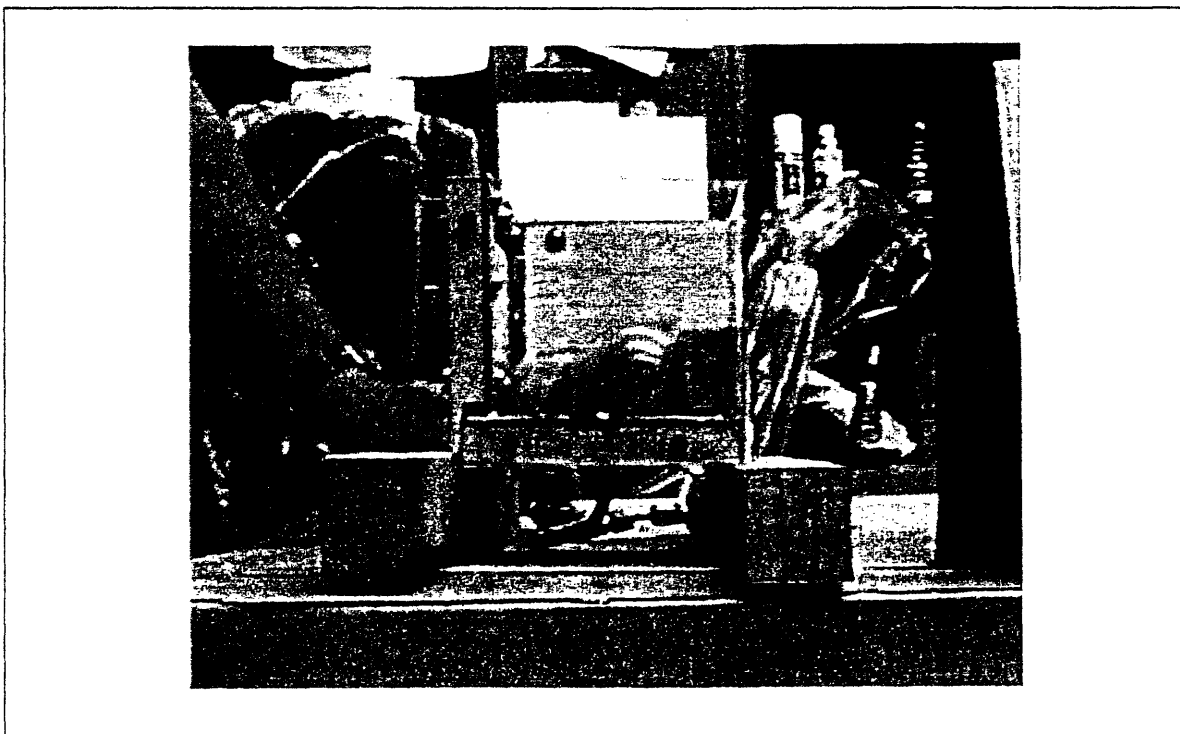
Figure 26: Side view of an internally constrained diaphragm with imbedded fabric expanding against a tool.
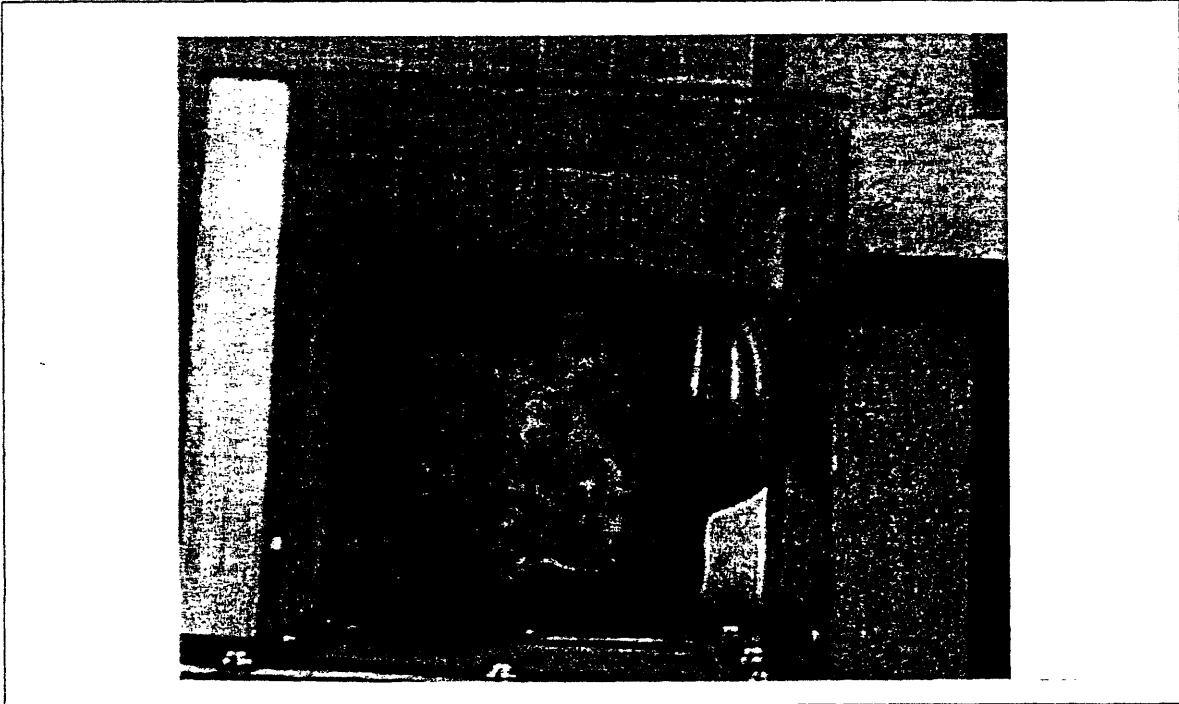
Figure 27: Top view of an internally constrained diaphragm with imbedded fabric expanding against a tool.

Conclusions

In these experiments, neither fluid inflation, nor the use of multiple diaphragms proved to be a feasible method of controlling the lower diaphragm in inflated tool forming. In order for fluid inflation to have a dramatic effect on diaphragm shape, the fluid density to diaphragm elasticity ratio would have to be very high. To achieve this, a heavy fluid such as mercury would have to be used in conjunction with a very thin membrane. The combination of rupture prone thin diaphragms and hazardous fluids is unattractive to manufacturing in comparison to other options. Multiple diaphragm inflation also has potential. With the right combination of thickness and sequence, dry diaphragms could be inflated to form a relatively flat surface for laminate loading. But the diaphragm interaction weakens as they are deflated during forming. This function of multiple diaphragm inflation would make it very hard to control the in-plane shear on the laminate during forming.

Using diaphragms with internal constraints is the most promising method of improving inflated tool forming. The threads give the diaphragm a clean, flat surface which will completely support the laminate during loading. The unconstrained portions of the diaphragm fill the gap between the tool and the diaphragm as has been illustrated in Figures 26 and 27. The ability of the threads to shape the diaphragm also opens the door to controlling the diaphragm during deflation. Since the threads control the surface by limiting vertical expansion, shortening the threads as pressure in the diaphragm decreases will maintain control. Thus dynamic threads must maintain

$$l_x < k_2 \frac{P_o x^4}{E t^3} \tag{9}$$

in order to maintain control of the diaphragm surface. Through active threads the user would have control over the tension in the diaphragm and thus the in-plane shear in the laminate.

Through the used of internally constrained diaphragms, it may be possible to create wrinkle free parts with high precision.

Appendix A
Empirical constants and definitions of R for expanding plates[4]
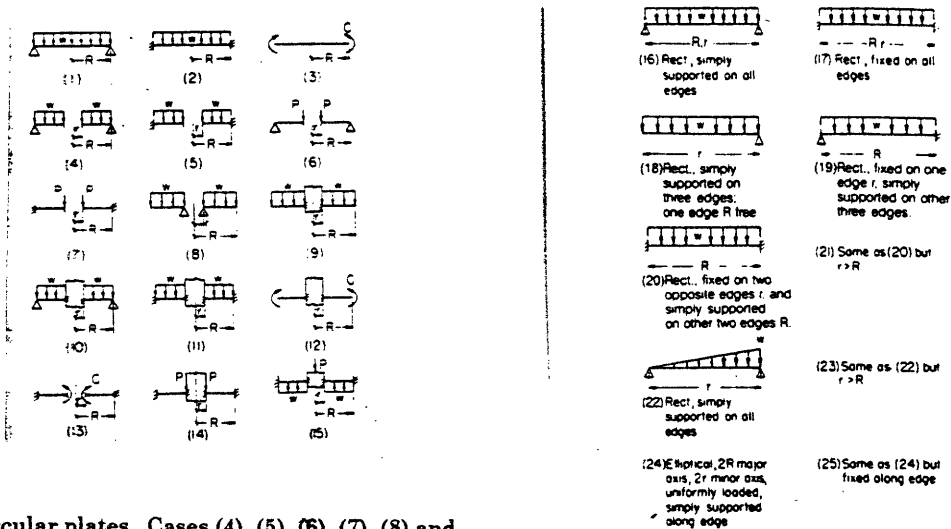
Circular plates. Cases (4), (5), (6), (7), (8) and (13) have central hole of radius r; cases (9), (10), (11), (12), (14), and (15) have a central piston of radius r to which the plate is fixed

Rectangular and eliptical plates. [R is the longer dimension except in cases (21) and (23)

Case	k	k₁
1	1.24	0.696
2	0.75	0.171
3	6.0	4.2

	R/r										
	1.25		1.5		2		3		4		5	
Case	k	k₁	k	k₁	k	k₁	k	k₁	k	k₁	k	k₁
4	0.592	0.184	0.976	0.414	1.440	0.664	1.880	0.824	2.08	0.830	2.19	0.813
5	0.105	0.0025	0.259	0.0129	0.481	0.057	0.654	0.130	0.708	0.163	0.730	0.176
6	1.10	0.341	1.26	0.519	1.48	0.672	1.88	0.734	2.17	0.724	2.34	0.704
7	0.195	0.0036	0.320	0.024	0.455	0.081	0.670	0.171	1.00	0.218	1.30	0.238
8	0.660	0.202	1.19	0.491	2.04	0.902	3.34	1.220	4.30	1.300	5.10	1.310
9	0.135	0.0023	0.410	0.0183	1.04	0.0938	2.15	0.293	2.99	0.448	3.69	0.564
10	0.122	0.00343	0.336	0.0313	0.740	0.1250	1.21	0.291	1.45	0.417	1.59	0.492
11	0.072	0.00068	0.1825	0.005	0.361	0.023	0.546	0.064	0.627	0.092	0.668	0.112
12	6.865	0.2323	7.448	0.6613	8.136	1.493	8.71	2.555	8.930	3.105	9.036	3.418
13	6.0	0.196	6.0	0.485	6.0	0.847	6.0	0.940	6.0	0.801	6.0	0.658
14	0.115	0.00129	0.220	0.0064	0.405	0.0237	0.703	0.062	0.933	0.092	1.13	0.114
15	0.090	0.00077	0.273	0.0062	0.710	0.0329	1.54	0.110	2.23	0.179	2.80	0.234

Coefficients for Circular Plates

	R/r									
	1.0		1.5		2.0		3.0		4.0	
Case	k	k₁	k	k₁	k	k₁	k	k₁	k	k₁
16	0.287	0.0443	0.487	0.0843	0.610	0.1106	0.713	0.1336	0.741	0.1400
17	0.308	0.0138	0.454	0.0240	0.497	0.0277	0.500	0.028	0.500	0.028
18	0.672	0.140	0.768	0.160	0.792	0.165	0.798	0.166	0.800	0.166
19	0.500	0.030	0.670	0.070	0.730	0.101	0.750	0.132	0.750	0.139
20	0.418	0.0209	0.626	0.0582	0.715	0.0987	0.750	0.1276	0.750	
21*	0.418	0.0216	0.490	0.0270	0.497	0.0284	0.500	0.0284	0.500	0.0284
22	0.160	0.0221	0.260	0.0421	0.320	0.0553	0.370	0.0668	0.380	0.0700
23*	0.160	0.0220	0.260	0.0436	0.340	0.0592	0.430	0.0772	0.490	0.0908
24	1.24	0.70	1.92	1.26	2.26	1.58	2.60	1.88	2.78	2.02
25	0.75	0.171	1.34	0.304	1.63	0.379	1.84	0.419	1.90	0.431

* Length ratio is r/R in cases 21 and 23.

Coeficients for rectangular and eliptical plates

---

[4] From Marks' Standard Handbook for Mechanical Engineers 10th Edition pg 5-48 to 5-50

Appendix B
Stills created from the video documenting these experiments in diaphragm control

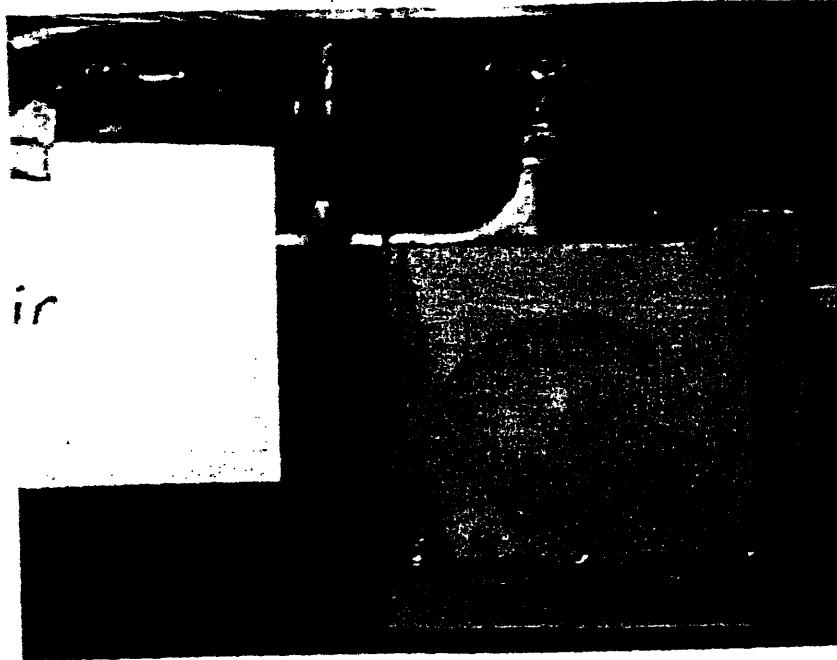t_H = Horizontal Thickness, t_v = Vertical Thickness

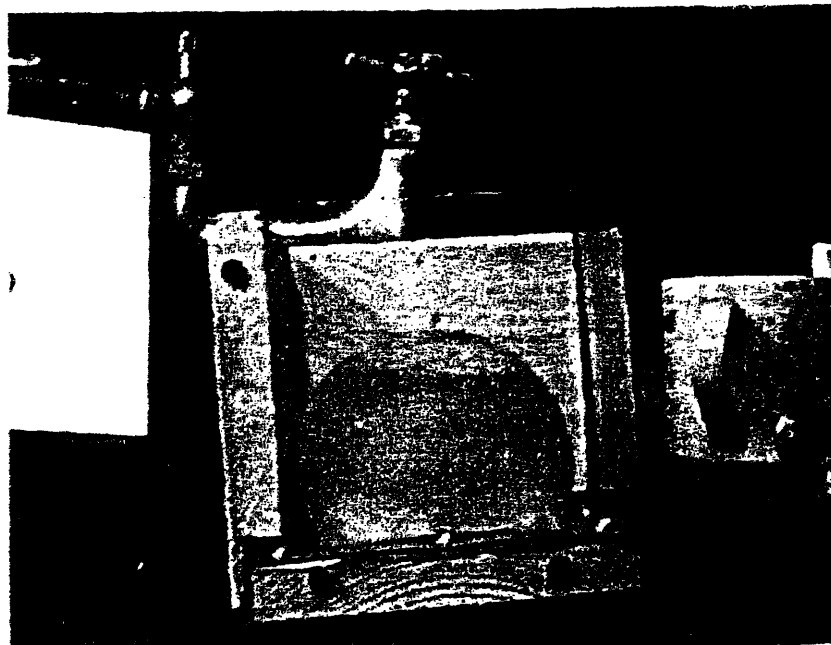Figure 28: t_H = $\frac{1}{50}$" Fluid = Air; density = 24 $^{kg}/_{m^3}$
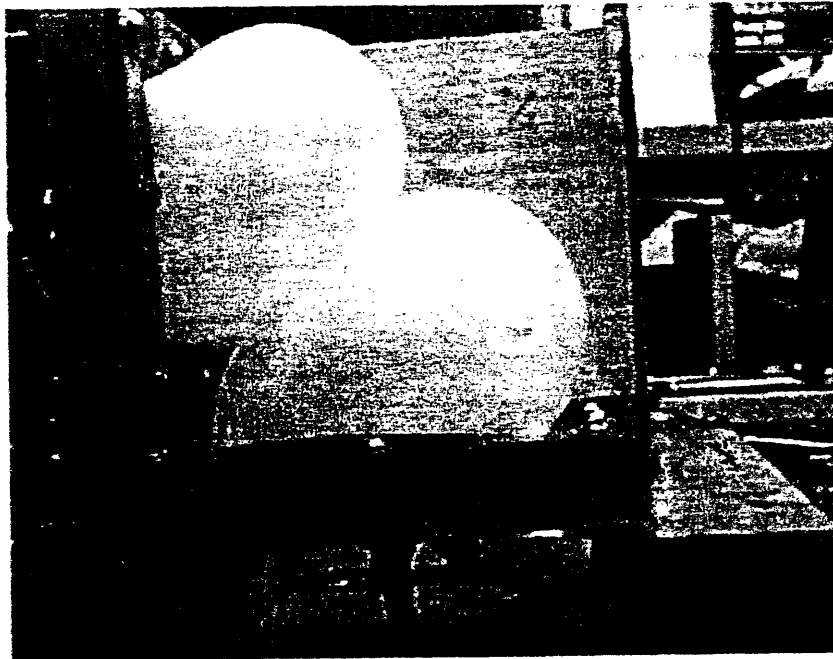

Figure 30: Fluid = Water; density = 1000 $^{kg}/_{m^3}$

Figure 31: $t_H = \frac{1}{50}$" $t_H = \frac{1}{50}$" Inflated Together, Dry Interface

Figure 32: $t_H = \frac{1}{50}$" $t_H = \frac{1}{50}$" Inflated Together, Dry Interface
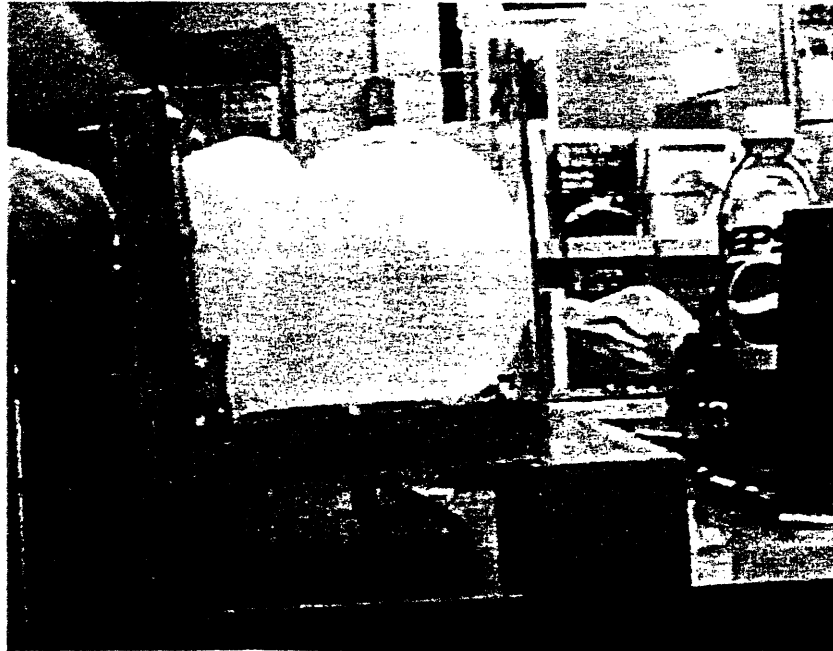
Figure 33: $t_H = 1/50$" $t_H = 1/50$" Horizontal First Dry Interface
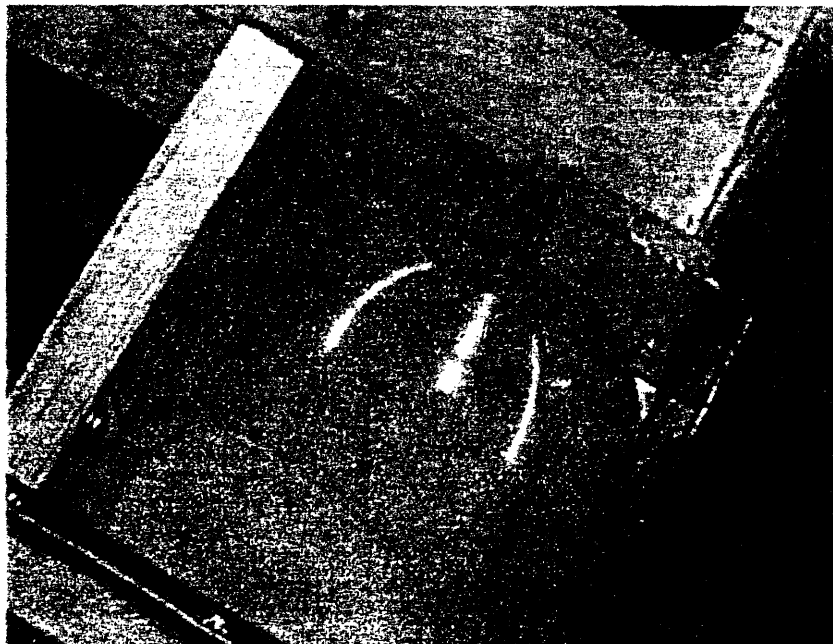
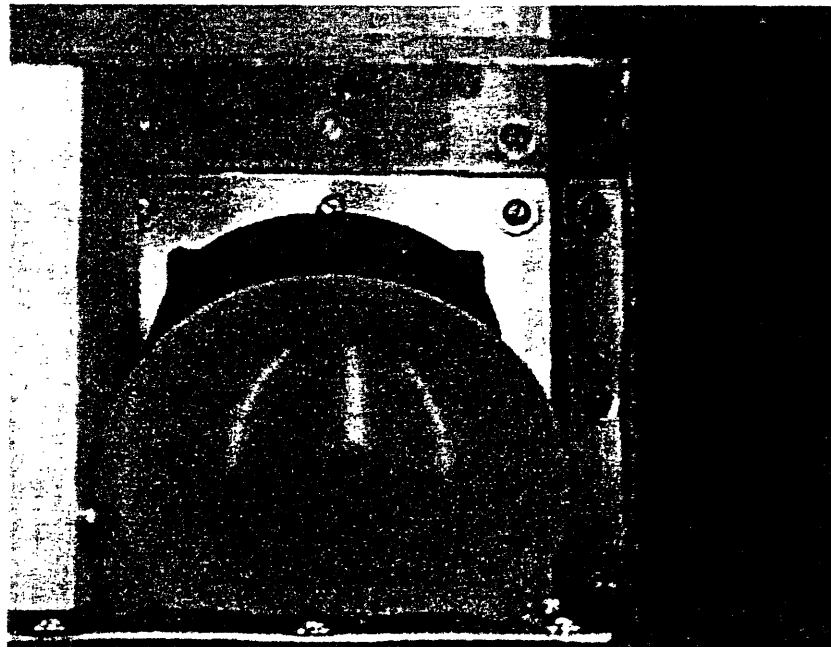Figure 34: $t_H = 1/50$" $t_H = 1/50$" Horizontal First Dry Interface

33
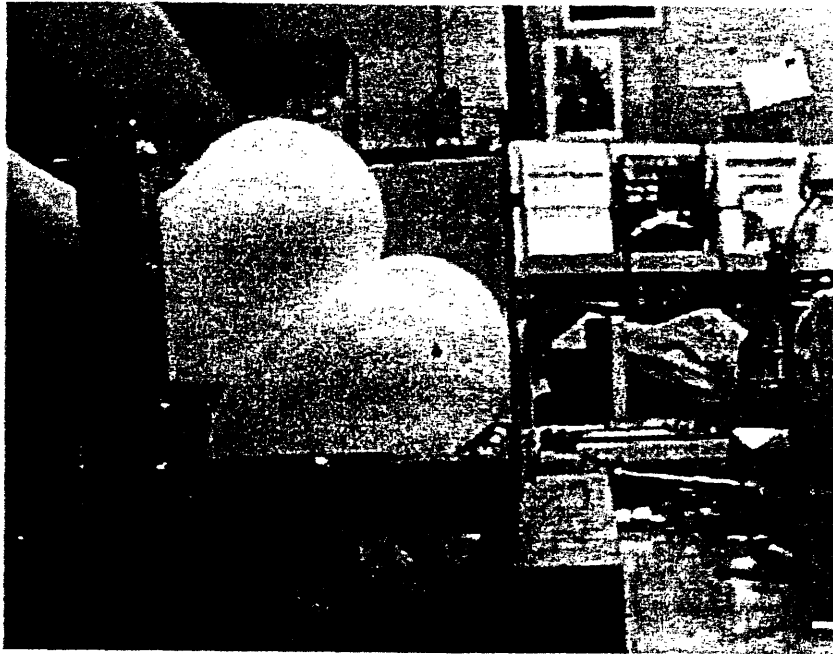
Figure 35: $t_H = \frac{1}{50}$" $t_H = \frac{1}{50}$" Vertical First Dry Interface
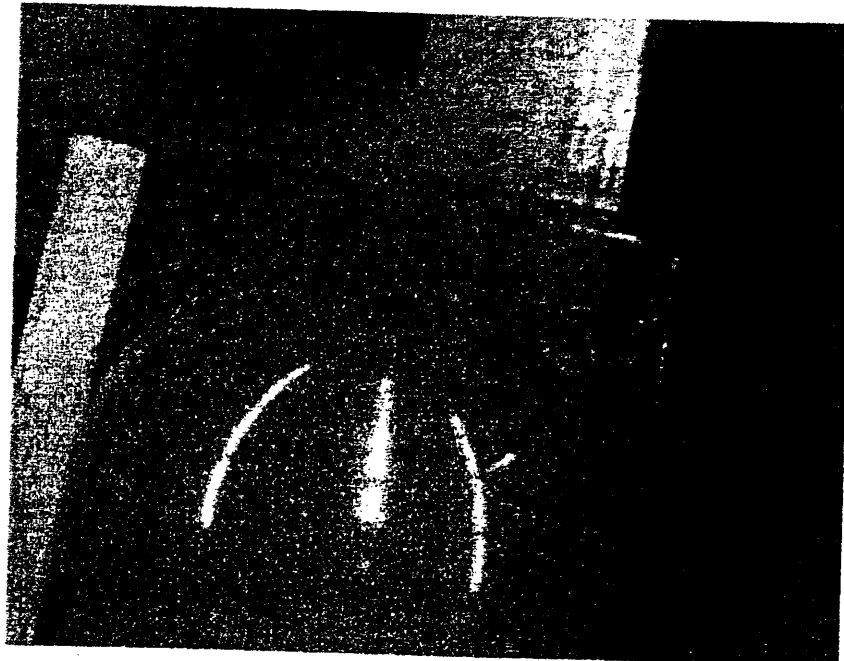
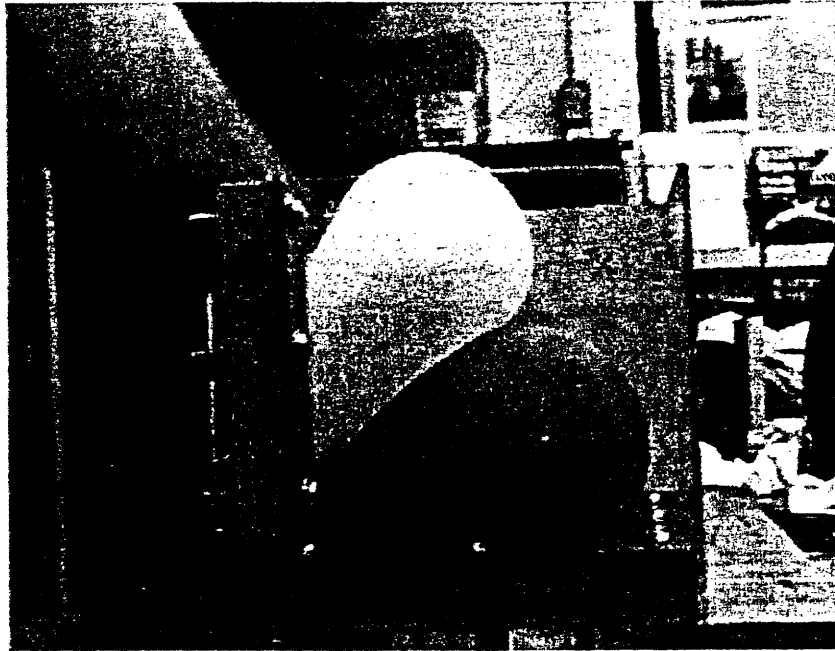Figure 36: $t_H = \frac{1}{50}$" $t_H = \frac{1}{50}$" Vertical First Dry Interface
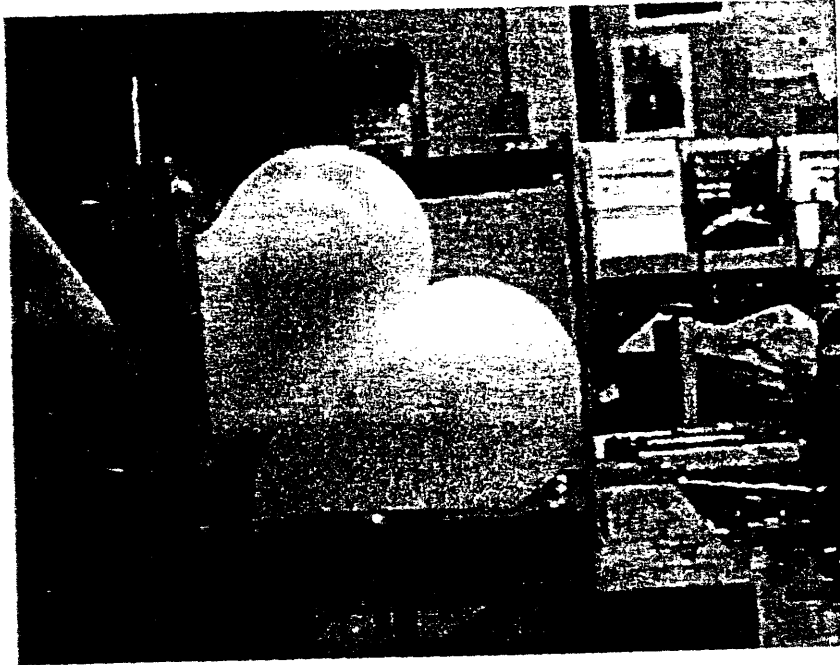
Figure 37: $t_H = 1/50"$ $t_H = 1/50"$ Inflated Together, Petroleum
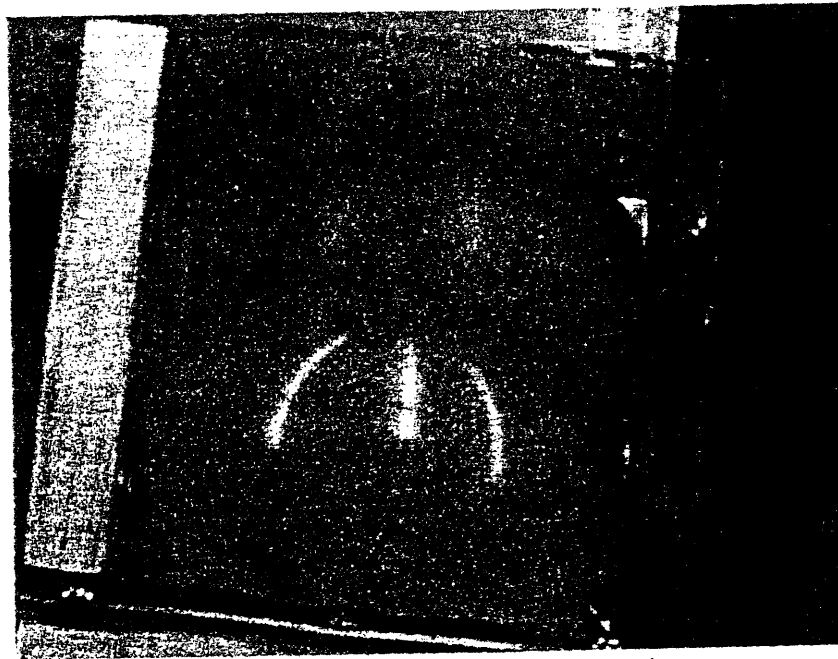
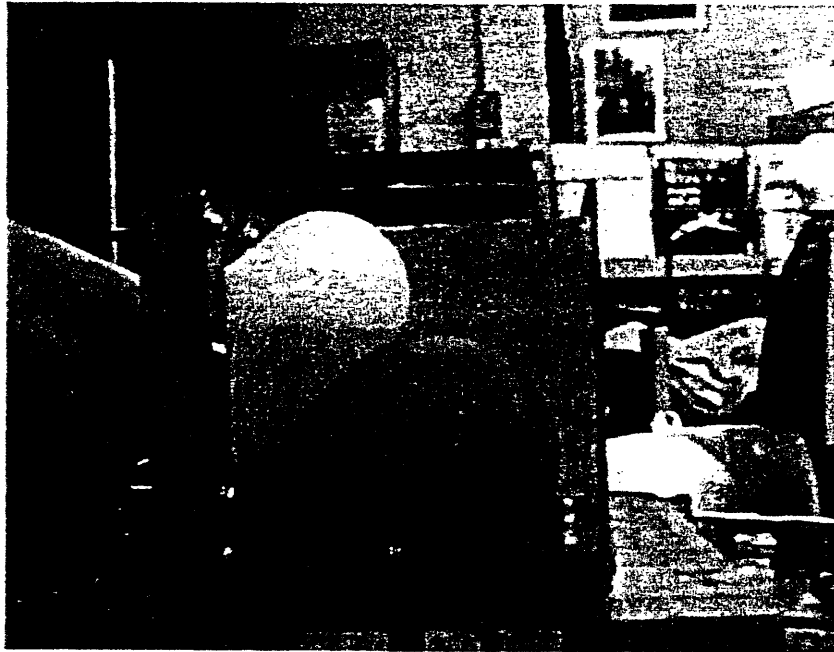Figure 38: $t_H = 1/50"$ $t_H = 1/50"$ Inflated Together, Petroleum

Figure 39: $t_H = \frac{1}{50}$" $t_H = \frac{1}{50}$" Horizontal First, Petroleum
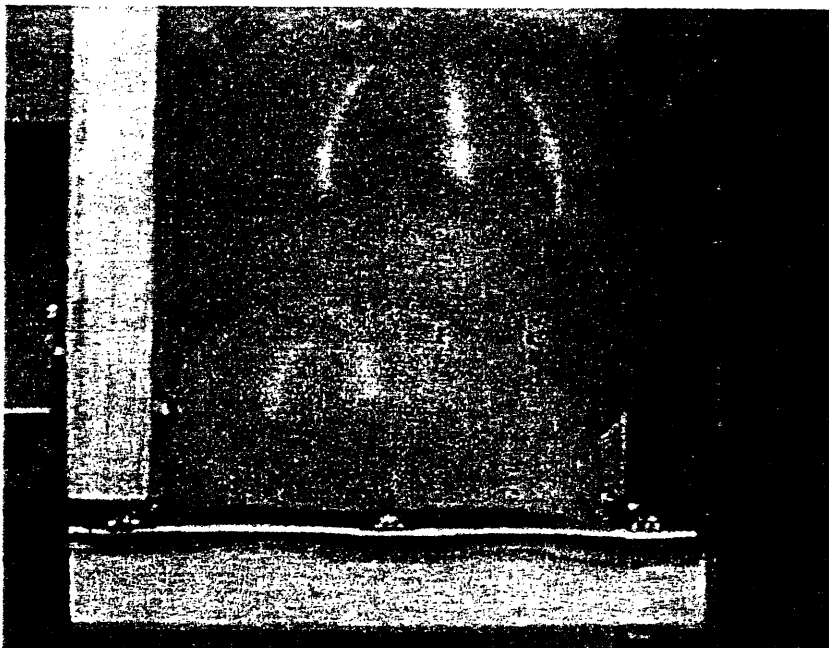
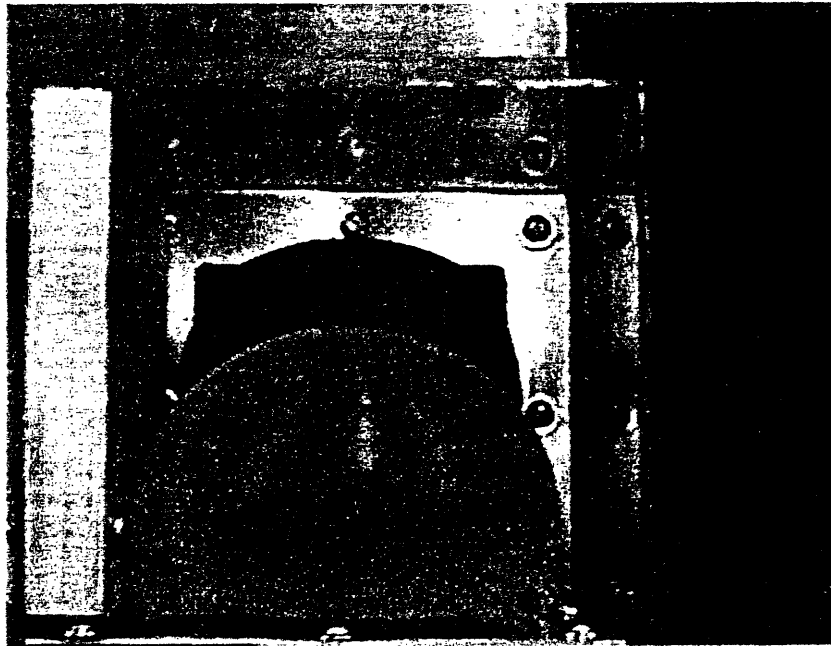Figure 40: $t_H = \frac{1}{50}$" $t_H = \frac{1}{50}$" Horizontal First, Petroleum
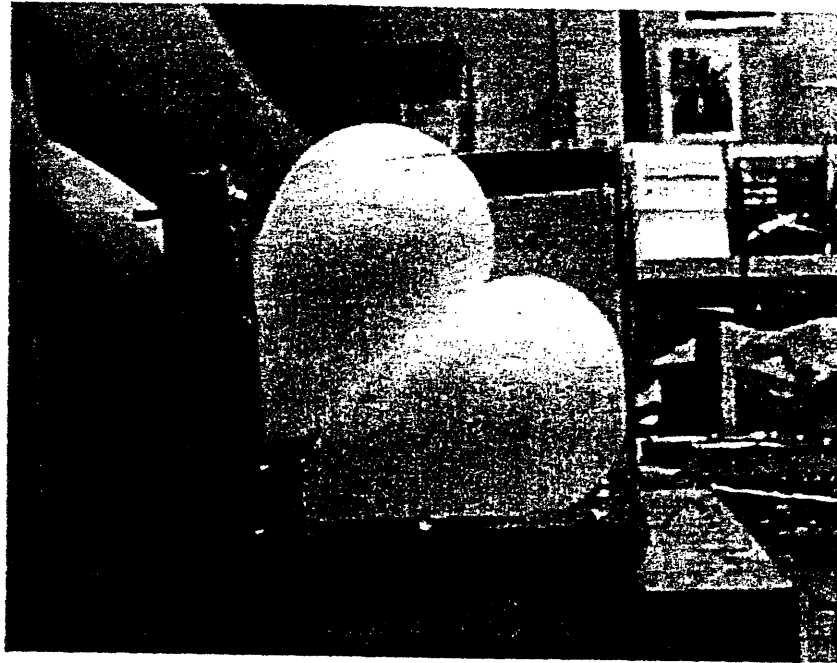
Figure 41: $t_H = 1/50$" $t_H = 1/50$" Vertical First, Petroleum

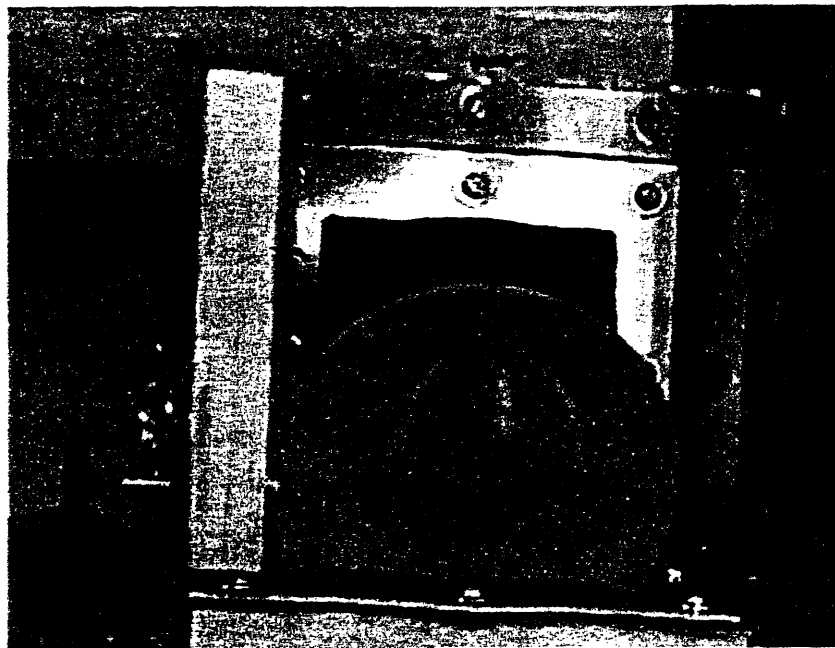Figure 42: $t_H = 1/50$" $t_H = 1/50$" Vertical First, Petroleum

Figure 43: t_H = $^1/_{16}$" t_H = $^1/_{50}$" Inflated Together, Dry Interface

Figure 44: $t_H = \frac{1}{16}$" $t_H = \frac{1}{50}$" Horizontal First, Dry Interface
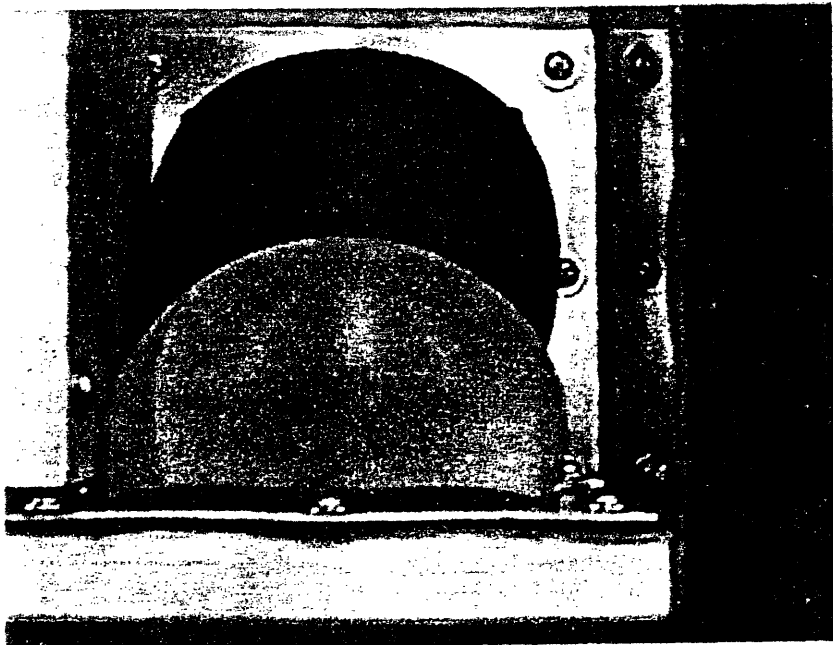
Figure 45: $t_H = \frac{1}{16}$" $t_H = \frac{1}{50}$" Horizontal First, Dry Interface
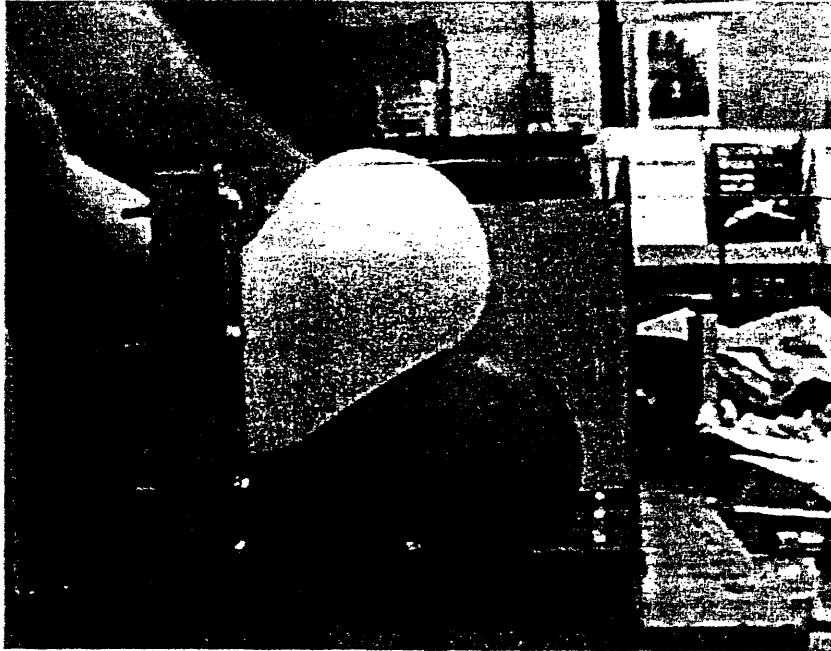
Figure 46: $t_H = \frac{1}{16}$" $t_H = \frac{1}{50}$" Vertical First, Dry Interface

Figure 47: $t_H = \frac{1}{16}$" $t_H = \frac{1}{50}$" Vertical First, Dry Interface

Figure 48: $t_H = \frac{1}{16}$" $t_H = \frac{1}{50}$" Inflated Together, Petroleum
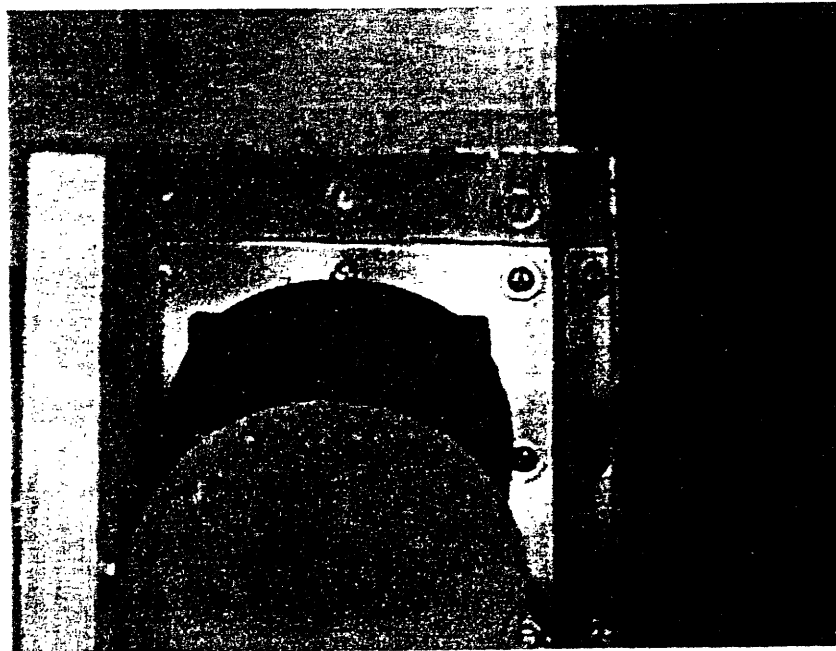
Figure 49: $t_H = \frac{1}{16}$" $t_H = \frac{1}{50}$" Inflated Together, Petroleum

Figure 50: $t_H = 1/16$" $t_H = 1/50$" Horizontal First, Petroleum

Figure 51: $t_H = 1/16$" $t_H = 1/50$" Horizontal First, Petroleum

Figure 52: t_H = $^1/_{16}$" t_H = $^1/_{50}$" Vertical First, Petroleum

Figure 53 t_H = $^1/_{16}$" t_H = $^1/_{50}$" Vertical First, Petroleum

Figure 54: $t_H = 1/50$" $t_H = 1/16$" Inflated Together, Dry Interface
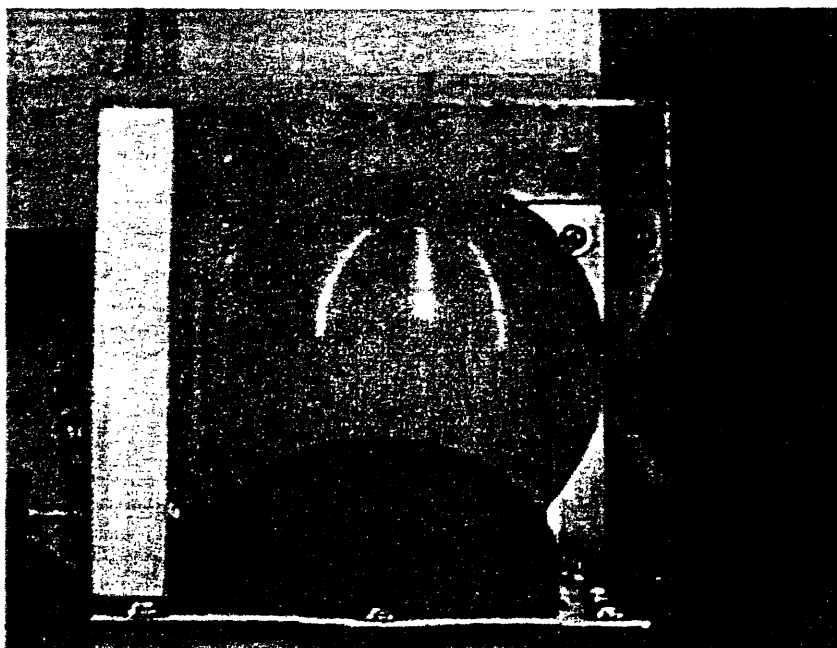
Figure 55: $t_H = 1/50$" $t_H = 1/16$" Inflated Together, Dry Interface

44

Figure 56: $t_H = \frac{1}{50}$" $t_H = \frac{1}{16}$" Horizontal First, Dry Interface

Figure 57: $t_H = \frac{1}{50}$" $t_H = \frac{1}{16}$" Horizontal First, Dry Interface

Figure 58: $t_H = \frac{1}{50}$" $t_H = \frac{1}{16}$" Vertical First, Dry Interface
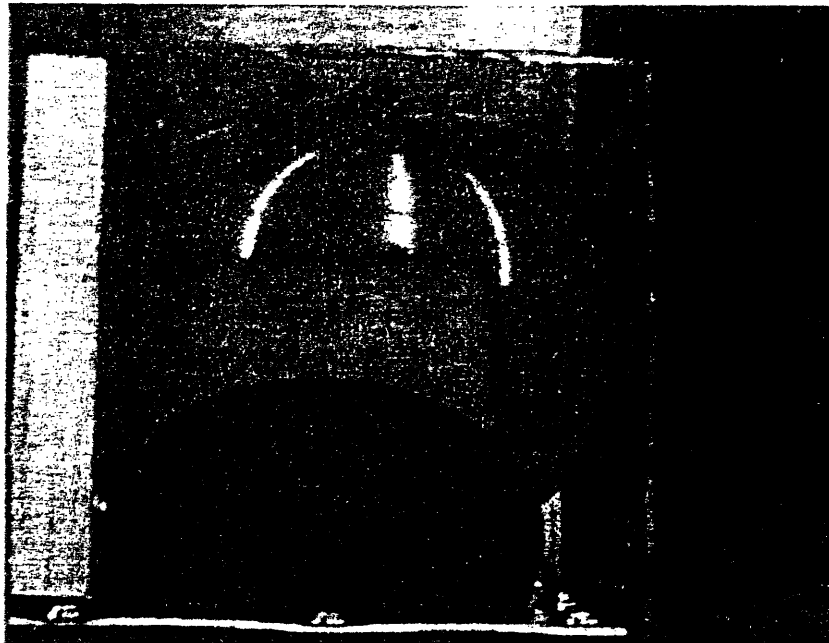
Figure 59: $t_H = \frac{1}{50}$" $t_H = \frac{1}{16}$" Vertical First, Dry Interface

Figure 60: $t_H = \frac{1}{50}$" $t_H = \frac{1}{16}$" Inflated Together, Petroleum
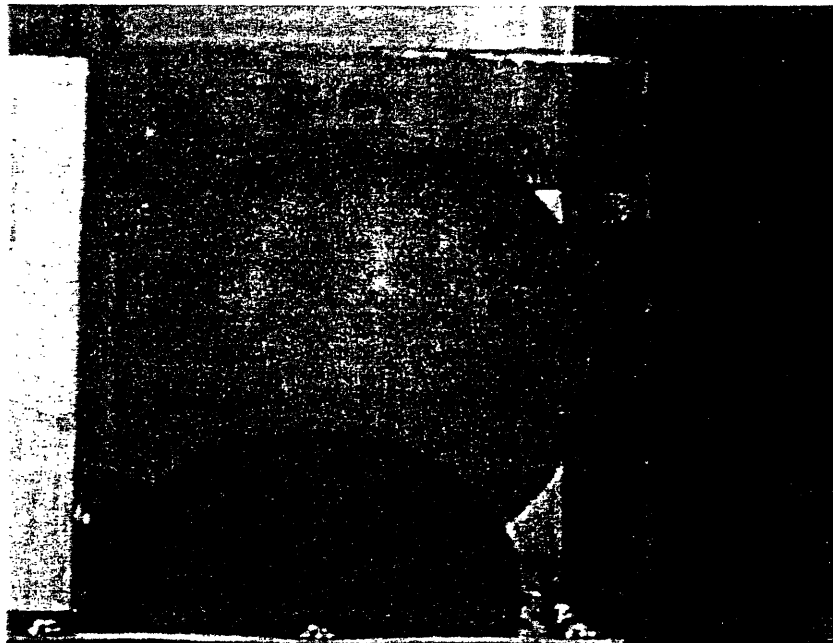
Figure 61: $t_H = \frac{1}{50}$" $t_H = \frac{1}{16}$" Inflated Together, Petroleum

Figure 62: $t_H = {}^1/_{50}$" $t_H = {}^1/_{16}$" Horizontal First, Petroleum
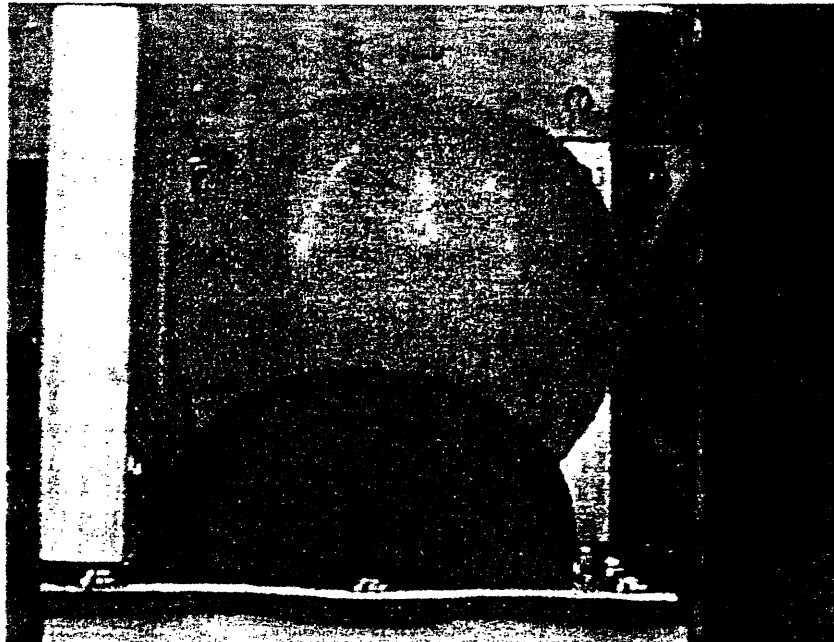
Figure 63: $t_H = {}^1/_{50}$" $t_H = {}^1/_{16}$" Horizontal First, Petroleum
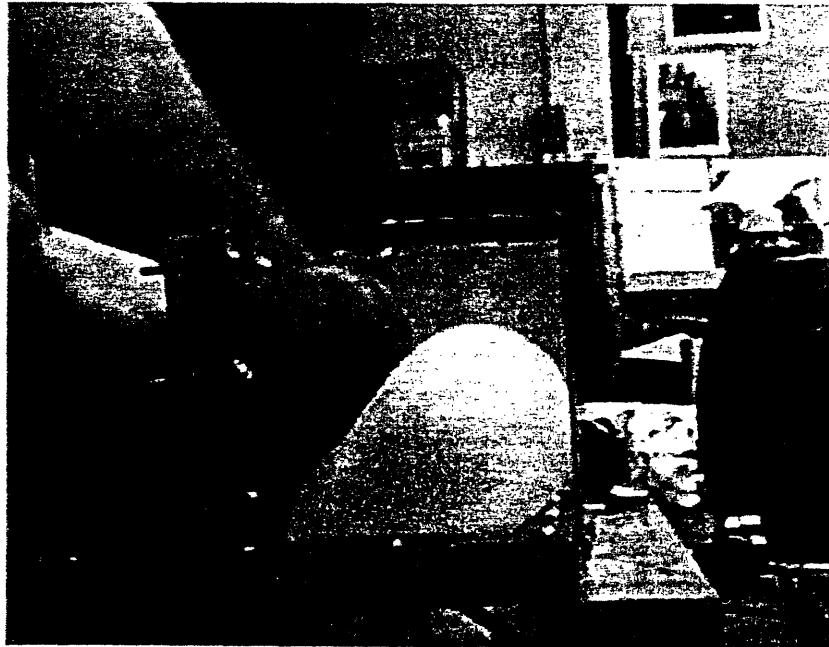
Figure 64: $t_H = \frac{1}{50}$" $t_H = \frac{1}{16}$" Vertical First, Petroleum
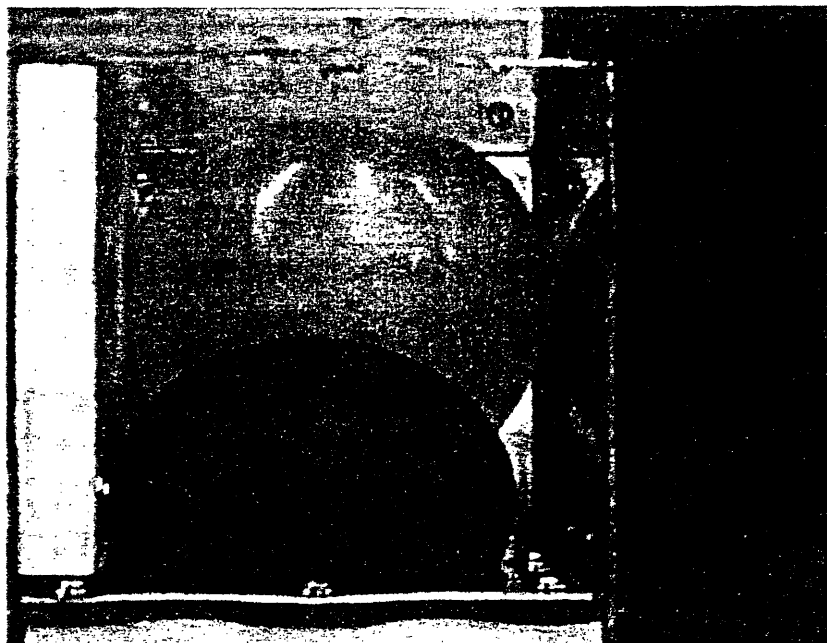

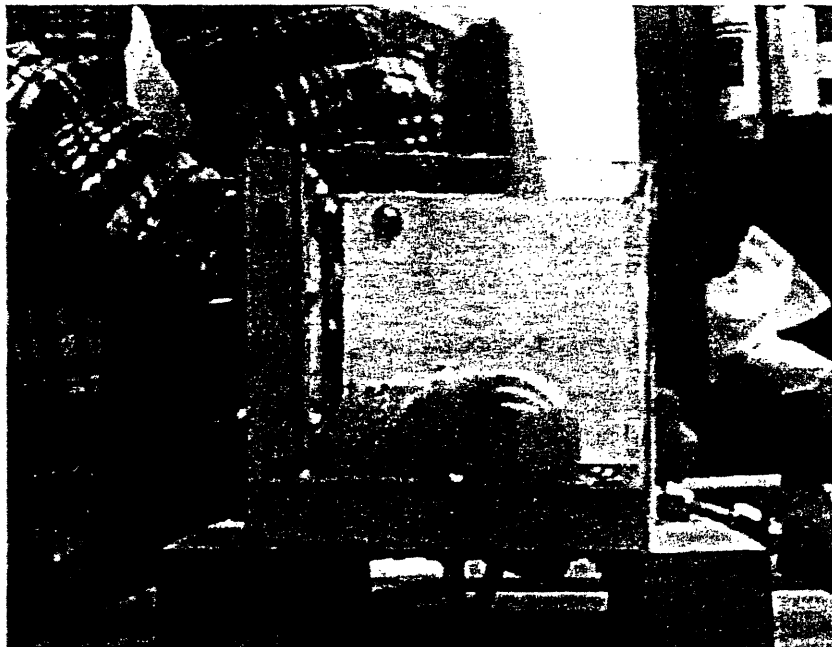Figure 65: $t_H = \frac{1}{50}$" $t_H = \frac{1}{16}$" Vertical First, Petroleum

Figure 66: Internally constrained diaphragm with imbedded fabric
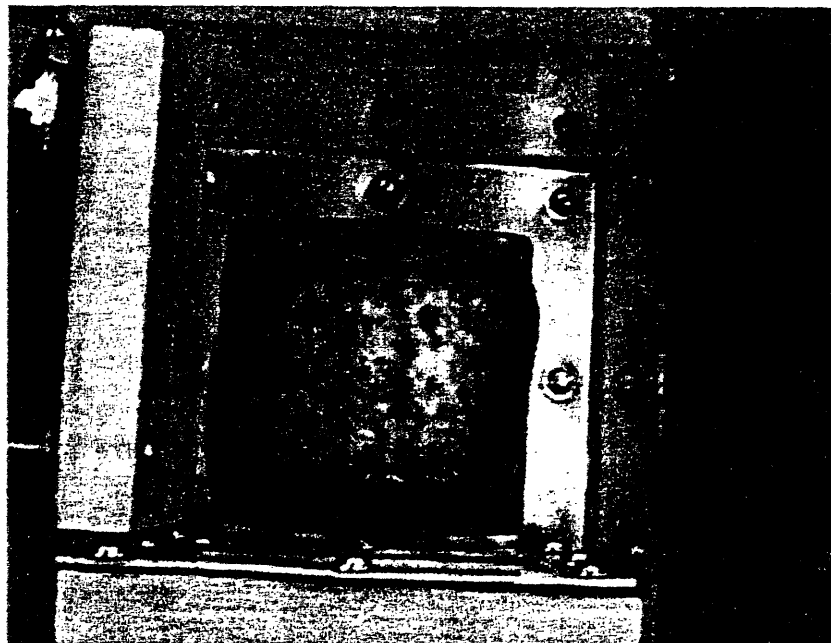

Figure 67: Internally constrained diaphragm with imbedded fabric

References

Tam, Albert S. & Timothy Gutowski, "The Kinematics for Forming Ideal Aligned Fibre Composites into Complex Shapes" Composite Manufacturing Vol. 1 No. 4 December 1990

Avallone, Eugene A. & Theodore Baumeister III, **Marks' Standard Handbook for Mechanical Enginees** 10th Edition, McGraw-Hill, New York, NY 1996